TURUN YLIOPISTO

N, N-dimethoxy-aminals as dynamic pH-responsive ligations for oligonucleotides

Master's Thesis in Exact Science

University of Turku

Department of Chemistry

Master's Degree Programme in Chemistry of Drug Development

July 2025

Mahdieh Mozaffari Majd

The originality of this thesis has been checked in accordance with the University of Turku quality assurance system using the Turnitin Originality Check service.

Master's thesis

Subject: Department of Chemistry, MDP in Exact Science, Chemistry of Drug Development

Author: Mahdieh Mozaffari Majd

Title: *N, N*-dimethoxy-aminals as dynamic pH-responsive ligations for ONs

Supervisors: Prof. Pasi Virta, Dr. Heidi Korhonen, Prof. Tuomas Lönnberg

Abstract

Dynamic covalent chemistry harnesses the reversible formation of chemical bonds and provides a powerful approach for designing stimuli-responsive biomolecular systems[1]. This study aims to develop and evaluate a novel pH-sensitive linker, *N,N*-dimethoxy-2,2-bis(aminomethyl)propane-1,3-diol, for its integration into ONs through its terminal and interchain modifications.

As outlined in Scheme 1, two synthetic strategies were established: (A) Immobilization onto a solid support for automated DNA synthesis, and (B) Conversion into a phosphoramidite building block for solid-phase synthesis. A DMTr-cation assay confirmed successful loading of solid support, and ONs modified via both pathways were obtained on the micromole scale.

The modified linker was successfully introduced at both the terminal and intrachain positions of the ONs, including hairpin-forming sequences. Due to its flexible structure and ability to form reversible bonds, the linker is well suited to the construction of adaptive, stimuli-sensitive nucleic acid systems. This work demonstrates the viability of *N, N*-dimethoxy-aminal linkers as pH-sensitive ligation tools in oligonucleotide design.

Keywords: Dynamic Covalent Chemistry, pH-responsive linker, Reversible aminal, Base filling-element, ON Synthesis

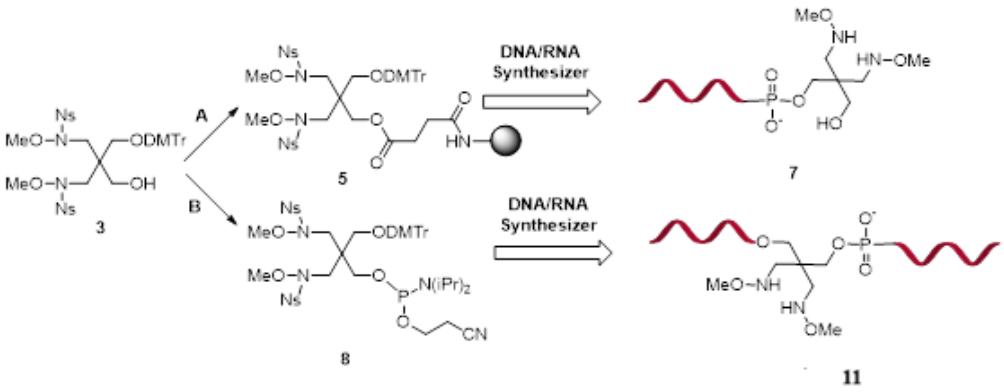

Scheme 1 Overview of the two Synthetic Strategies for Incorporating *N, N*-dimethoxy-2,2-bis(aminomethyl)propane-1,3-diol

Preface

This master's thesis was carried out as part of my studies in the Chemistry of Drug Development program at the University of Turku. The research was conducted in the Bioorganic Research Group under the guidance of Prof. Pasi Virta, Dr. Heidi Korhonen, and Prof. Tuomas Lönnberg, whose expertise and encouragement have been invaluable throughout this process. I wish to express my sincere thanks for their support, insightful feedback, and mentorship.

I also extend my appreciation to the colleagues and staff of the research group and laboratory, whose collaborative spirit and willingness to help contributed significantly to the completion of this work.

This work is dedicated to my family, my husband, and our two children, whose unwavering encouragement and understanding have supported me through every phase of this academic journey.

Table of Contents

List of abbreviations

Abbreviation	Definition
BTT	5-Benzylthio-1-H-tetrazole
CPG	Controlled Pore Glass
DBU	1,8-Diazabicyclo[5,4,0] undec-7-ene
DCC	Dynamic Covalent Chemistry
DCL	Dynamic Combinatorial Library
DIAD	Diisopropyl azodicarboxylate
DIPEA	*N, N*-Diisopropylethylamine
DMAP	4-Dimethylaminopyridine
DMF	Dimethylformamide
DMTr	4,4'-Dimethoxytrityl
DMTrCl	4,4'-Dimethoxytrityl Chloride
DMSO	Dimethyl sulfoxide
ESI-TOF HRMS	Electrospray Ionization – Time-of-Flight High Resolution Mass Spectrometry
HPLC	High-Performance Liquid Chromatography
LC/MS	Liquid Chromatography-Mass Spectrometry
LNA	Locked Nucleic Acid
MOANA	N-Methoxy-1,3-oxazinane nucleic acid
NMR	Nuclear Magnetic Resonance
Nosyl	p-Nitrobenzenesulfonyl
ON	ON
OTS	ON-templated synthesis
Py	Pyridine
ROS	Reactive Oxygen Species
RP-HPLC	Reverse-Phase High Performance Liquid Chromatography
siRNA	Small Interfering RNA
TEA	Triethylamine
TEAA	Triethyammonium acetate

Abbreviation	Definition
TCA	Trichloroacetic Acid
THF	Tetrahydrofuran
TLC	Thin Layer Chromatography
UV-Vis	Ultraviolet-Visible Spectrometry

1 Introduction

1.1 Stimuli-responsive systems in drug delivery and nanotechnology

Smart materials are molecular systems that dynamically alter their properties, such as solubility or conformation, in response to environmental signals. Their responsiveness is often reflected in shifts in solubility, conformational dynamics, reversible covalent bonding, or stimulus-triggered release of bioactive agents. The core principles of stimulus-responsiveness lie in conditional activation: the material remains stable and inert under normal physiological conditions but undergoes a structural or chemical transformation upon encountering a specific stimulus. This functionality can e.g. reduce off-target of drugs and enhance therapeutic precision. For example, a drug carrier may remain intact during blood circulation but release its cargo in response to the acidic environment of a tumour or reductive cytosolic conditions inside cells. In drug delivery applications, stimuli-responsiveness ensures that therapeutic cargo is only released in targeted regions, thereby improving treatment efficacy and minimizing off-target effects[2-7].

As shown in Figure 1,after endocytosis, nanocarriers encounter various internal and external stimuli, such as acidic pH, high glutathione (GSH) concentration, and light-triggered site-specific drug release within subcellular compartments (e.g., cytosol and nucleus)[8]. These smart systems enhance therapeutic precision by exploiting the unique microenvironment of diseased cells.

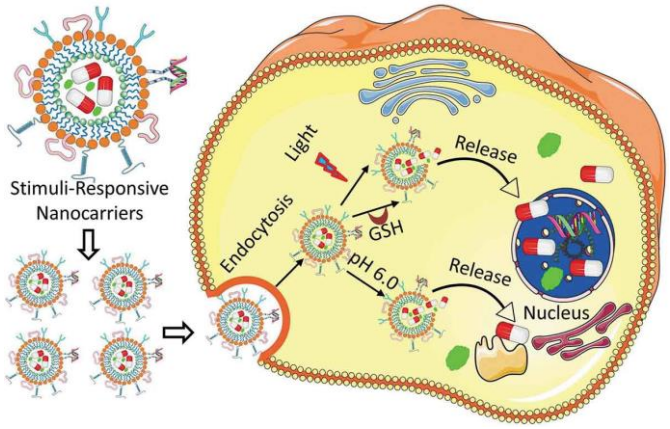

Figure 1 Schematic representation of stimuli-responsive nanocarriers for intracellular drug delivery [8].

1.1.1 Types of Stimuli

Stimuli triggering responses in these systems are typically divided into two main classes: internal (endogenous) and external (exogenous) stimuli[9].

- **Internal Stimuli (Biological Triggers)**

  These arise from the physiological environment and are particularly relevant in biomedical contexts:

- pH gradients: observed between intracellular compartments (e.g., endosomes, lysosomes) or in pathological sites like tumors and inflamed tissues
- Redox potential: High concentration of glutathione (GSH) in the cytosol vs. the extracellular environment
- Enzymatic activity: Tissue- or disease-specific enzymes (e.g., esterases, proteases)
- Reactive oxygen species (ROS): Elevated in cancer or inflammatory conditions
- Glucose levels: used in diabetes-responsive systems

- **External Stimuli (User-Controlled Triggers)**

  These allow precise spatial and temporal control over activation:

- Temperature: Causing sol-gel transition or polymer collapse
- Light: Including bond cleavage (e.g., photolabile groups) or isomerization (e.g., azobenzene switches)

- Magnetic fields: Activating nanoparticles for remote targeting
- Ultrasound: Facilitating cavitation permeability enhancement
- Electric Fields: Modulating electrophoretic transport or redox-responsive systems

1.2 Importance of pH-responsive systems

Among the various stimuli studied in smart materials, pH has become one of the most versatile and biologically significant triggers. Its variability across cellular compartments and disease states enables highly targeted applications, especially in drug delivery and molecular diagnostics. Because pH can be measured non-invasively and shows predictable differences between diseased and healthy tissues, it is a valuable basis for designing responsive systems based on dynamic covalent chemistry.

pH plays a critical regulatory role in biological systems and serves as a key stimulus for the design of responsive materials. Different cellular compartments and tissue environments maintain distinct pH levels, forming natural gradients that can be exploited for targeted drug delivery, diagnostics, and molecular switching. For example, the cytosol typically maintains a neutral pH of ~ 7.2, while acidic organelles such as endosomes and lysosomes exhibit pH values ranging from 4.5 to 6.5. These gradients have been successfully harnessed in numerous drug delivery strategies to trigger controlled release or structural activation of pH-sensitive systems[10].

In pathological contexts, pH gradients are even more pronounced. Tumour tissues often exhibit an acidic extracellular pH (~ 6.5-6.8) due to elevated glycolysis and lactic acid secretion (Warburg effect), while the intracellular environment remains near-neutral. This differential has been used to guide the release of chemotherapeutics from pH-sensitive carriers.

pH-responsive nanoparticles leverage the acidic tumor microenvironment to trigger drug release through multiple physicochemical mechanisms. Drug-loaded pH-sensitive nanoparticles accumulate in tumor tissues characterized by mildly acidic pH (~ 6.5). The acidic conditions trigger drug release through mechanisms such as (1) acid-responsive swelling, (2) solubility changes, (3) changes in modulation, and (4) cleavage

of acid-labile covalent bonds. This strategy enables targeted and controlled release within pathological environments[10].

Inflammation sites, ischemic tissues, and wounds similarly display reduced pH due to localized hypoxia and metabolic stress. During the acute inflammation phase, wound pH can drop to ~ 5-6 before rising toward neutral or alkaline values (~ 7-8) as healing progresses or becomes chronic[11].

Additionally, microbial infections often acidify their surrounding environment, offering another biologically relevant trigger for pH-responsive systems. Bacteria, especially in biofilm-forming communities, metabolize glucose and other nutrients into acidic byproducts such as lactic acid, formic acid, and acetic acid. These secreted metabolites progressively lower the local pH-often reaching values as low 5.0 -5.5 in infected tissues or at the implant interface. The acidic microenvironment is further reinforced by the host immune response: activated neutrophils and macrophages release acidic granules and produce reactive oxygen species (ROS), which also contribute to local acidosis[12].

The following table summarizes pH values across various biological and disease-related microenvironments:

Table 1 pH values in selected biological compartments and pathological sites

Compartment Tissue	Typical pH Ranges	Notes
Cytosol	~ 7.2	Neutral intercellular environment
Nucleolus	~ 7.2	Similar to Cytosol
Endosomes	5.5-6.5	Acidification in the early-to-late transition
Lysosomes	4.5-5.0	Strongly acidic; hydrolytic activity
Tumour extracellular space	6.2-6.9	Acidic due to glycolysis
Inflammation sites	6.0- 6.8	Acidosis from immune cell activity
Wound environment	5.4- 7.0	Dynamic depending on the stage of healing
Bacterial infections	5.5- 6.5	Local acidification by microbial metabolism

These distinct microenvironments serve as the foundation for designing pH-sensitive systems using dynamic covalent linkers. Oxazolidines and *N, N*- dimethoxy-aminals - both of which respond to mildly acidic pH - are excellent candidates for integration into DNA nanostructures, drug carriers, and biosensors targeting these compartments. Their reversible formation and hydrolysis offer programmable functionality that is tightly coupled to the cellular or tissue-specific landscape.

1.3 Importance of oligonucleotides in responsive drug delivery systems

As illustrated in Figure 2, the development of oligonucleotide (ON) therapeutics has progressed from fundamental discoveries in DNA structure to advanced clinical applications, including antisense ON (ASOs), siRNA, and aptamers. This technological evolution has established ONs as a new class of therapeutics, forming the third

cornerstone of current drug development strategies. Unlike traditional drugs that often target proteins via active binding pockets, ONs can modulate gene expression at the nucleic acid level through sequence-specific hybridization to RNA or DNA, enabling them to address otherwise “undruggable” targets[13].

Recent advancements in ON chemistry - such as phosphorothioate backbones, 2’-O modification, locked nucleic acids (LNAs), and bioconjugation - have improved stability, target affinity, and in vivo performance. These chemical strategies have led to a new generation of ONs capable of resisting nuclease degradation while retaining or enhancing target engagement, ultimately translating into better pharmacokinetic profiles and reducing dosing frequency. The most widely used chemical modifications for therapeutic ONs are , including backbone, sugar, and base modifications that improve nuclease resistance and cellular uptake [14].

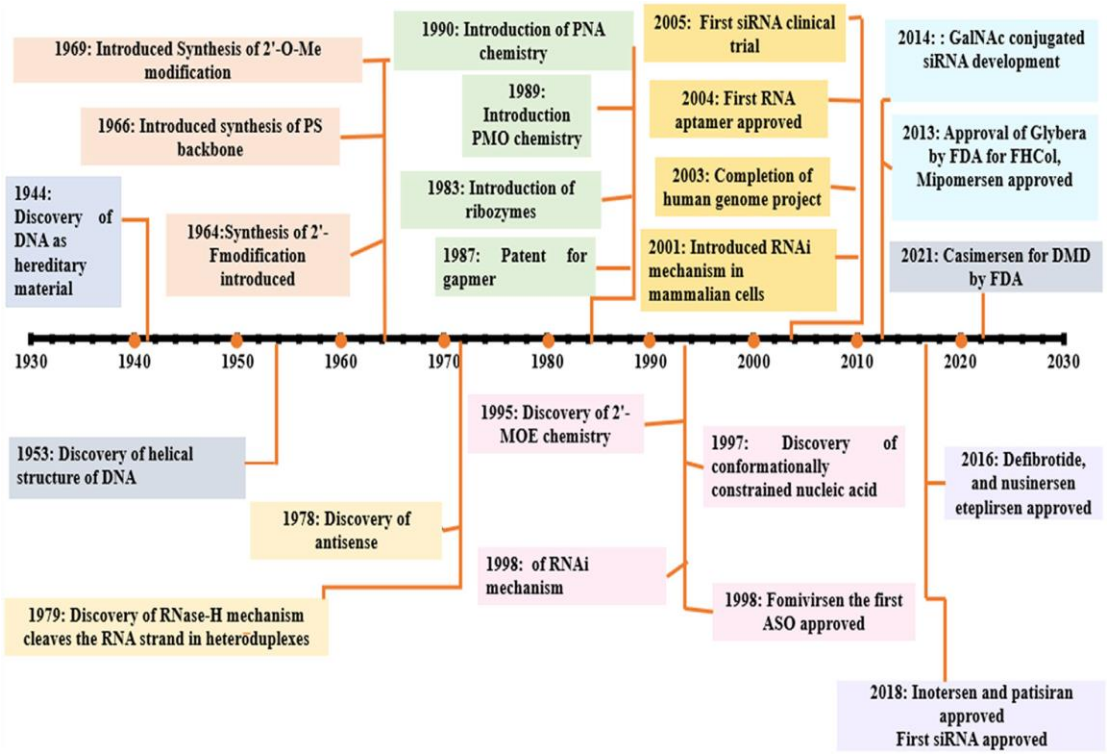

Figure 2 Timeline of key historical milestones in the development of ON therapeutics, from the discovery of DNA as a hereditary material to the latest FDA approvals of siRNA drugs and antisense ONs [18]

Despite these innovations, delivery remains a major bottleneck for the clinical translation of ON therapeutics. Several strategies have been explored, including lipid nanoparticles, aptamer-functionalized carriers, and stimuli-responsive scaffolds[15]. Stimuli-responsive systems, particularly those based on dynamic covalent chemistry (DCC), provide a means to trigger drug release under specific physiological conditions such as acidic tumour microenvironments or redox gradients [15]. DNA nanostructures have proven to be an excellent vehicle for ON-based therapies due to their intrinsic biocompatibility, design flexibility, and addressability. Figure 7 highlights common DNA architectures, such as duplexes, G-quadruplexes, and i-motifs, which play crucial roles in structural switching, cargo release, and pH responsiveness[16, 17].

Furthermore, the incorporation of G-quadruplexes and i-motifs introduces secondary structural responsiveness, allowing for pH-sensitive switching and regulated cargo release. These motifs, used in reconfigurable nanodevices and logic gates, enhance the precision of drug delivery applications and open new frontiers in intelligent therapeutics[17].

From a clinical perspective, several ON drugs have already reached the market, and hundreds of ONs are in late-stage clinical trials targeting neurological cardiovascular and metabolic diseases. The continuous expansion of this field, particularly through advances in responsive delivery systems and customization strategies, underscores the critical role of ONs in the next generation of precision medicine[18, 19].

1.4 Principles of dynamic covalent chemistry in nucleic acid engineering

Dynamic Covalent Chemistry (DCC) has emerged as a promising strategy in synthetic and biological chemistry, enabling the design of molecular systems that combine the robustness of covalent bonding with the reversibility of noncovalent interactions. As its core, DCC exploits reversible bonds that form and break under thermodynamic control, allowing chemical systems to self-assemble, reorganize, and adapt in response to environmental cues. This approach stands in contrast to traditional covalent chemistry,

which typically yields static products. Instead, DCC systems exist in equilibrium and can undergo structural changes dynamically when exposed to changes in conditions[1, 20, 21].

The conceptual foundation of DCC lies in dynamic combinatorial libraries (DCLs), where a set of building blocks interconvert through reversible covalent reactions to form a mixture of products. The equilibrium compositions of these libraries can shift in response to external stimuli, making them particularly useful for the discovery of new receptors, ligands, or catalysts[22]. In biology, this dynamic adaptability is attractive for designing responsive systems that mimic natural processes like enzyme regulation, signal transduction, and cellular feedback loops.

DCC's relevance to biology has expanded significantly with the advent of dynamic biomaterials and biorthogonal reactions. In drug delivery, DCC principles are used to design systems that release therapeutic agents in response to the acidic environment of tumour tissue or the reducing conditions inside cells[23, 24]. Stimuli-responsive hydrogels based on reversible covalent crosslinks can change their mechanical properties in situ, enabling controlled drug release, cell encapsulation, or tissue engineering applications[25]. Meanwhile, in synthetic biology, dynamic covalent motifs have been employed to construct programmable molecular devices and logic gates that respond to physical signals[26].

When applied to nucleic acid chemistry, DCC provides a versatile framework for creating dynamic DNA- and RNA-based materials that can respond to their environment in a predictable and programmable manner. This is particularly valuable in applications where structural changes such as hybridization, folding, or strand displacement are essential for function. DCC expands the chemical toolbox available for such applications, allowing reversible control over ON interactions and structure. This has proven useful in the development of biosensors, molecular logic devices, responsive aptamers, and targeted delivery systems[21, 27].

1.5 Reversible covalent linker for nucleic acids: from imines to aminals

Several types of reversible covalent bonds have been explored, each with different stabilities, reactivities, and suitability under different conditions[1]. Among the reversible linkages explored , imines are some of the simplest, formed by condensation of aldehydes with amines. However, their instability in an aqueous environment limits their use in physiological conditions. Hydrazones and oximes, derived from hydrazines and hydroxylamines, respectively, provide better hydrolytic stability and are favoured for their biocompatibility, although their formation is often slow and requires acidic catalysis or electron-rich aldehydes[1, 28].

Disulfide linkers have long been utilized in redox-responsive ON systems due to their ability to be cleaved in the reducing environment of the cytosol[29]. Similarly, boronic esters provide reversible covalent binding with diols and have been employed in sugar-sensing applications. Nevertheless, their aqueous instability and synthetic limitations constrain their widespread use[30].

In contrast, oxazolidines have shown great promise due to their balance of stability and responsiveness. These five-membered cyclic linkers form through the reaction of 2-amino alcohols with aldehydes, resulting in a heterocycle containing both nitrogen and oxygen in the ring, Scheme 2. Their structure resembles a substituted 1,3-oxazinane, which can undergo reversible ring-opening in response to mildly acidic environments[31, 32]. The formation is reversible and can be triggered or reversed by tuning pH, and remains stable at neutral pH around 7.4, but is readily hydrolyzed under acidic conditions, making it suitable for pH-triggered bond cleavage[33]

Oxazolidines possess several features that make them suitable for ON modification. They exhibit hydrolytic stability under neutral to slightly basic conditions, while still enabling cleavage under acidic conditions typical of endosomal or tumour microenvironments. Their cyclic geometry allows for compact and rigid integration into DNA and RNA structures, making them useful for generating stable but responsive linkages in modular nanodevices, hairpins, or junctions. Additionally, the reaction

conditions for forming oxazolidine are compatible with automated synthesis and post-synthetic modification, which facilitates their use in ON design. The Bioorganic research group at the University of Turku has developed a series of pH-responsive ON ligations using oxazolidine linkage[33-35]. These systems have been used to construct split aptamers and base-modified aptamers post-SELEX, demonstrating improved binding diversity and adaptability[36]

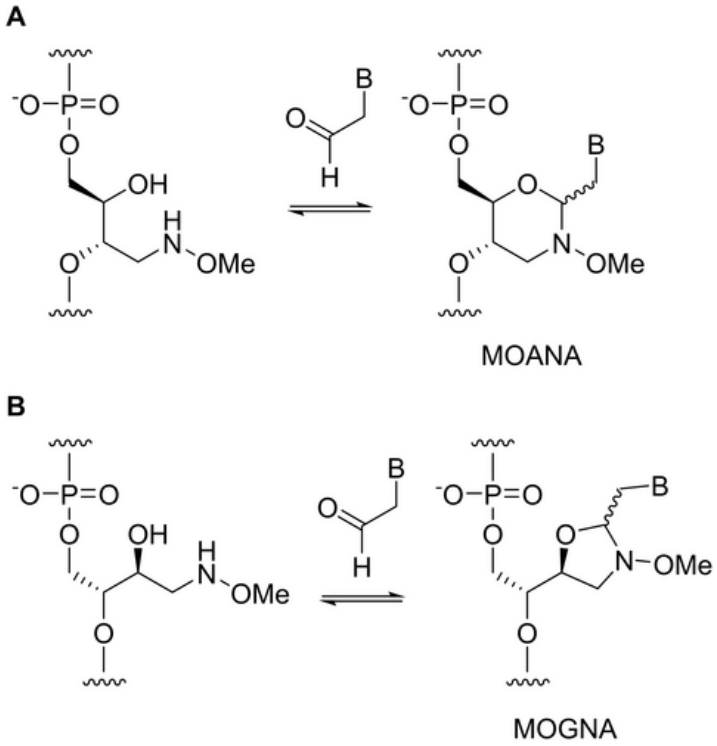

Scheme 2 Dynamic N, O-heterocycles oxazinane and oxazolidine (6-membered, 5-membered heterocycles) formation on a nucleoside backbone through methoxyamine-aldehyde condensation [32]

While oxazolidine has proven effective, new chemistries are continuously explored to expand the toolbox of reversible linkers. Aminals represent a novel class of compounds with potential for dynamic ON ligation. These structures are formed by the reaction of

aldehydes with primary or secondary amines, producing a central carbon bound to two nitrogen atoms [37].

Their ability to undergo reversible hydrolysis under acidic conditions has made them attractive tools in supramolecular chemistry and emerging biomedical applications[38, 39].

A subset of aminals, *N, N*-dimethoxy aminals, can be considered as a useful tool for ON applications. These are formed through the condensation of aldehydes with dimethoxyamine. The methoxy substituent contributes to the stability of the linkage under neutral pH by delocalizing electron density and protecting the carbon from nucleophilic attack. They can act as compact, non-hydrogen bonding "base-filling" elements since they occupy the approximate spatial volume of a nucleobase, suitable for incorporation in bulges, loops, or terminal regions without inducing significant steric or conformational stress. Their symmetric structure possibly facilitates compatibility with automated synthesis protocols.

1.6 Oligonucleotide-templated synthesis and dynamic assembly

Oligonucleotide-templated synthesis (OTS) is a well-established technique that uses the sequence-specific hybridization of nucleic acids to guide chemical reactions. By aligning reactive groups on complementary strands, ONs serve as programmable scaffolds that bring reagents into close spatial proximity, thereby enhancing reaction efficacy and selectivity. This mimics biological information transfer processes, such as DNA replication and transcription, where precise base pairing dictates the outcome of enzymatic processes[40, 41]. OTS enables chemical transformation to occur under mild, aqueous conditions and with high sequence specificity, making it a valuable tool in molecular diagnostics, targeted prodrug activation, and nucleic acid engineering. In many applications, reactivity is contingent upon hybridization to a specific template strand, ensuring that reactions proceed only in the presence of the desired sequence.

This concept is illustrated Scheme 3. In the absence of a complementary nucleic acid template, reactive groups are diluted in solution and remain unreactive. Upon binding to a target DNA or RNA sequence, the effective molarity of the reagents increases due to spatial proximity enforced by the nucleic acid template on the nucleic acid scaffold. This templated proximity enables site-specific reactions, such as conversion of prodrugs into bioactive molecules or the uncaging of fluorophores in response to specific sequences. As shown in Scheme 3, nucleic acid-templated chemistry enables sequence-specific chemical control by bringing two chemical groups attached to separate probes into proximity through hybridization to adjacent sites on a specific DNA or RNA strand. This spatial agreement, guided by the target sequence, facilitates chemical transformations only in the presence of correct nucleic acids, ensuring precise and selective reactivity[41].

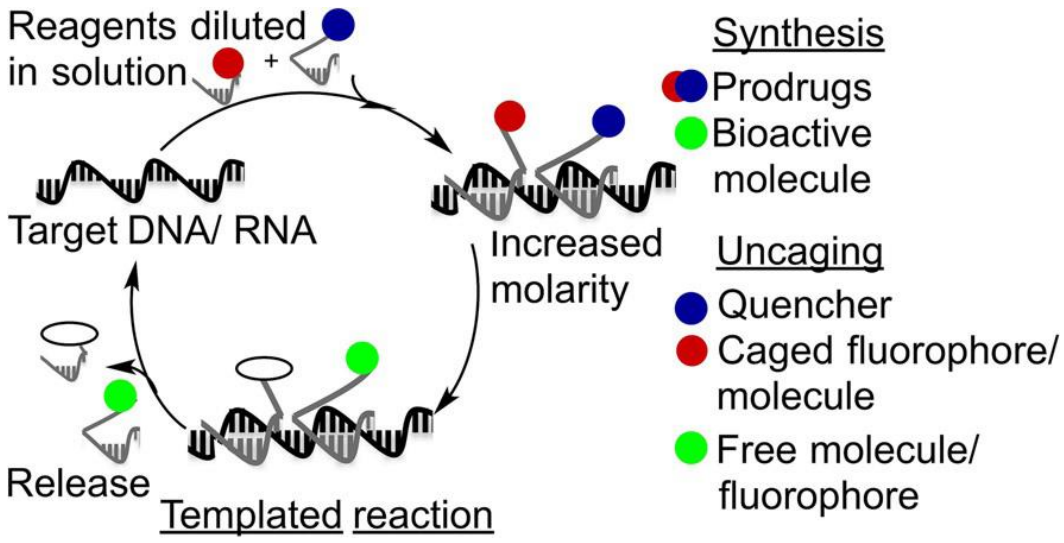

Scheme 3 Mechanism of ON-templated reactions for synthesis and uncaging applications [41]

In the context of dynamic covalent chemistry (DCC), OTS has enabled the formation of reversible linkages such as hydrazones, oximes, and aminals directly on DNA or RNA scaffolds. Recent works by Aho et al. (2022) showed that *N,O*-transacetalization of N-methoxyoxazolidine can be efficiently guided by hybridized ONs, with both formation and cleavage accelerated under mildly acidic conditions[35]. In this thesis, the templated ligation of *N, N*-dimethoxyaminal linker was explored in two structural contexts: (1) a

5’-terminally modified T4 ON and (2) a hairpin-structured ON bearing the linker. Once formed, the animal linker acts as a base-filling unit that supports the local architecture while remaining stable under neutral conditions.

1.7 Importance of base-filling design in dynamic ON systems

The idea of base-filling originated with the work of 1998 by Hickman, Sreenivasachary, and Lehn[42], and was formally named by Heemstra and Liu in 2009[43]. Base-filling is a strategy where artificial base-like units are inserted into ONs to take the place of natural nucleobases at specific sites, Scheme 4. These units form standard Watson-Crick base pairs but are designed to fit into the helical structure of DNA or RNA. This allows the strands to keep their shape while adding new chemical functions, such as pH-sensitivity or reversible bonding.

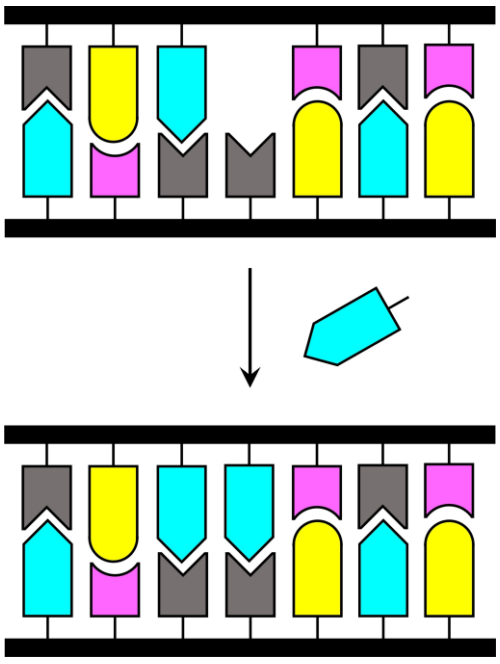

Scheme 4 Schematic illustration of the base-filling concept in a double-helical nucleic acid [31]

In dynamic nucleic acid systems, incorporating chemical linkers into loops, bulges, or abasic sites can disrupt local base-pairing and destabilize the duplex structure if poorly designed. Base-filling linkers overcome these challenges by mimicking the spatial volume of a nucleobase, helping to maintain proper spacing between neighboring bases and reducing structural distortion-without participating in base-pairing interactions. (preventing base-stacking). This approach is useful for engineering stimuli-responsive ON that undergo structural changes without compromising global stability. Oxazolidines[33] or oxazinanes [44] are introduced as reversible base-filling units that can be efficiently inserted into ONs at abasic sites and maintain structural integrity while enabling environmental responsiveness. In the present study, *N, N*-dimethoxy aminal linkers were employed as base-filling units in ON structures. Their tetrahedral center and symmetric structure allow them to occupy the place of a canonical base in non-pairing regions while introducing acid-labile cleavage sites. Under mildly acidic conditions, the C-N bond undergoes hydrolysis without the need for enzymatic assistance, making this linker system suitable for pH-triggered stand cleavage or conformational control. By incorporating linkers that do not hybridize but are structurally compatible with DNA, this design allows for the creation of ON structures that can respond in a controlled manner, such as releasing a drug. This base-filling approach combines the structural precision of natural DNA with the flexibility of dynamic covalent chemistry.

1.8 Scope and objective of this research

Among the various DCC strategies, the integration of acid-labile linkers into nucleic acid offers a promising platform for developing responsive nanostructures and controlled release systems.

This thesis focuses on the design, synthesis and characterization of dynamic ON constructs incorporating *N, N*-dimethoxy aminal linker. This linker can potentially act as a reversible base-filling unit within defined positions of ONs, either at 5'- terminus or interchain position via solid phase synthesis. While pH-responsiveness was not evaluated in this study, its chemical structure suggests potential for controlled cleavage under mildly acidic conditions.

This work aims to expand the molecular toolbox for constructing dynamic nucleic acid systems by combining the programmability of ONs with the adaptive reactivity of reversible covalent linkers.

2 Materials and methods

2.1 General methods

All chemicals, solvents, and ON synthesis reagents (including phosphoramidite and solid supports) were purchased from commercial suppliers and were used without further purification unless otherwise stated. Solvents used in organic synthesis were dried over activated 4 Å molecular sieves. Solvents' dryness was confirmed using Karl Fischer coulometric titration. Milli-Q grade deionized water was used for all aqueous preparations. Triethylamine (Et_3N) was freshly distilled to prepare HPLC elution buffers.

The ONs were synthesized using ÄKTA Oligopolist Plus 10 DNA/RNA synthesizer.

Solvent removal was carried out using rotary evaporation under reduced pressure. Thin-layer chromatography (TLC) was used to monitor reactions, and small-molecule purification was performed via silica gel chromatography. Synthesized ONs were purified using reversed-phase high-performance chromatography (RP-HPLC).

The structures of all the synthesized compounds were confirmed by NMR and mass spectroscopy. ^{1}H, ^{13}C, ^{31}P NMR spectroscopy, HSQC, and COSY spectra were recorded on an Oxford 500 MHz NMR instrument.

Mass Spectra were acquired using Agilent 6120 LC/MS and Waters AQUITY RDa UPLC/MS systems.

2.2 Synthesis of pH-Responsive linker

2.2.1 Synthesis of mono-DMTr-protected pentaerythritol -Compound **2**

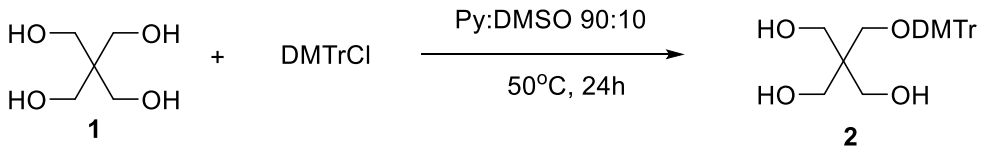

Scheme 5 Synthesis of Mono-DMTr-protected pentaerythritol

As shown in scheme 5, to begin the initial step toward synthesizing *N, N*-dimethoxy-2,2-bis(aminomethyl)propane-1,3-diol (**2**), pentaerythritol (8.0 g, 58.76 mmol, 5 eq) was dissolved in 350 mL of a 90:10 mixture of dried pyridine and DMSO. 4.0 g (11.34 mmol, 1eq) of 4,4-dimethoxyltrityl chloride (DMTrCl) was then added gradually in small portions. As the addition progressed, the reaction mixture turned yellow. The solution was stirred at 50 ℃ overnight to allow complete reaction. Once the reaction was complete, the solvent was removed. The resulting oily residue was dissolved in 100 mL of diethyl ether (Et_2O), followed by three sequential water extractions (3× 20 mL) to remove any remaining impurities. The organic layer was then dried over anhydrous sodium sulfate (Na_2SO_4), filtered, and evaporated to dryness. The purification step was particularly challenging, requiring careful separation to isolate the desired mono-DMTr-protected product. The crude product was purified through four successive silica gel chromatographies.

- The first purification was performed using a gradient elution system, starting from triethylamine (TEA): methanol (MeOH): dichloromethane (DCM) (0.5:10:89.5(*v*/*v*/*v*)) and gradually increasing to 0.5:20:79.5 (*v*/*v*/*v*). This step allowed effective initial separation of partially and fully substituted byproducts.
- The second purification was carried out with a gradient from TEA:MeOH: DCM (0.5:7.5: 89.5(*v*/*v*/*v*)) to 0.5: 15: 84.5(*v*/*v*/*v*), further enriching the target compound and removing overprotected species.
- The third purification used isocratic solvent system, TEA: MeOH: DCM (0.5:5:94.5(*v*/*v*/*v*))

- The final purification was conducted using TEA: n-hex: DCM starting (0.5: 30.5: 69(*v*/*v*/*v*)). Then, the solvent system was switched to TEA: MeOH: DCM, starting at 0.5:20:79.5 (*v*/*v*/*v*), which enabled high-purity isolation of mono-DMTr-protected product.

The final yield was 2.87 g (6.54 mmol), corresponding to a 56% isolated yield.

^{1}H NMR (500 MHz, $CDCl_3$): δ 6.8-7.4 (13H, aromatic H, DMTr group), 3.76 (6H, s, 2×OCH_3, DMTr group), 3.72 (6H, s, 3×CH_2OH), 3.13 (2H, CH_2ODMTr).

^{13}C NMR (126 MHz, $CDCl_3$): δ 160-110 (aromatic C, DMTr group); 86.3(CH_2ODMTr); 64.4, 63.9(CH_2OH); 55.2 OCH_3, DMTr group); 49.5(quaternary C).

HSQC (500 MHz, $CDCl_3$): Correlation signals conform to proton-carbon pairing for aromatic protons of DMTr group (7.24-7.38 ppm ↔ 127.4-129.8 ppm), methoxy groups (3.76 ppm↔55.8 ppm), methylene proton adjacent to oxygen (CH_2O and CH_2OH) (3.72, 3.88 ppm ↔ 64.4, 63.9)

ESI-TOF HRMS (ESI^+-TOF): *m/z* calc. for $[M+Na]^+$: 461.19 Da; Found: 461.1571 Da, *m/z* calc. for $[2M+Na]^+$: 899.39 Da; Found: 899.3514 Da.

2.2.2 Selective replacement of pentaerythritol hydroxyl groups by nosyl-protected methoxyamine-Compound **3**

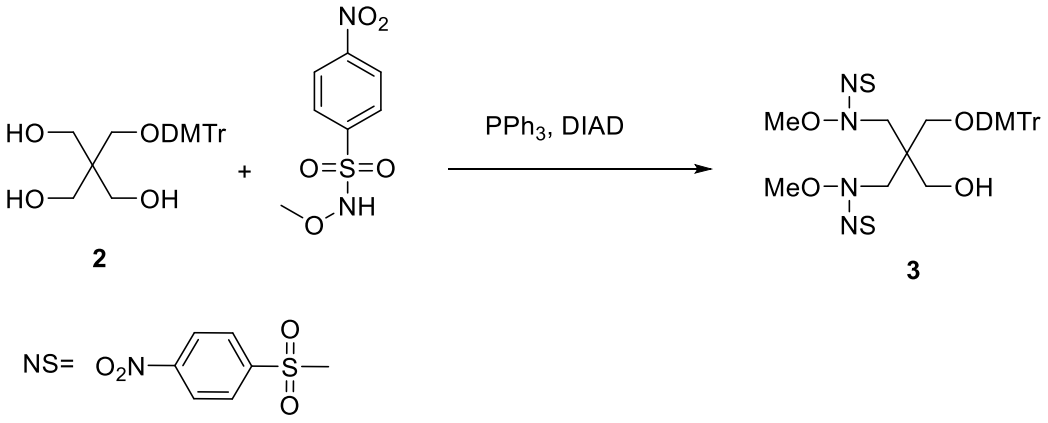

Scheme 6 Selective replacement of pentaerythritol hydroxyl groups by nosyl-protected methoxamine

To selectively protect two hydroxyl groups, as shown in Scheme 6, 2.00 g (4.56 mmol, 1 eq) of DMTr-pentaerythritol **2** was dissolved in 10 mL of dry tetrahydrofuran (THF). The solution was cooled to 0℃ using an ice bath. Then, 2.20 g (9.47 mmol, 2.1 eq) of *N*-methoxy-4-nitrobenzenesulfonamide (nosyl-protected *N*-methoxyamine), 2.50 g (9.53 mmol,2.2 eq) of triphenylphosphine (PPh_3), and 2.00 mL (10.09 mmol, 2.2 eq) of diisopropylazodicarboxylate (DIAD) were added dropwise under stirring. After 10 min, the ice bath was removed, and the reaction mixture was allowed to stir overnight at room temperature.

Following completion, the solvent was removed. Two successive silica gel column chromatographies purified the crude residue. The first was carried out using a gradient elution from TEA: EtOAc: DCM (0.5: 0:99.5(*v*/*v*/*v*)) to (0.5:10:89.5(*v*/*v*/*v*)). The second purification employed a gradient elution from TEA: EtOAc: n-hexane (0.5:25 74.5(*v*/*v*/*v*)) to (0.5:50:49.5(*v*/*v*/*v*)).

^{1}H NMR (500 MHz, $CDCl_3$): δ 8.33 (4H, d ,J=9Hz, aromatic H, ortho to NO_2), 7.96 (4H, d, J=9.Hz, aromatic H, meta to NO_2), 7.12-7.25 (9H, aromatic H, DMTr group), 6.7 (4H, aromatic H, DMTr group), 3.70 (6H, s, 2×OCH_3, DMTr group), 3.63 (2H, d, CH_2OH), 3.52 (6H, s, 2×CH_3O-N), 3.20 (2H, CH_2ODMTr), 3.18 (2H, CH_2-N), 2.90(2H, CH_2-N).

^{13}C NMR (126 MHz, $CDCl_3$): δ 158.6, 151.1, 144.1, 138.57, 135.3, 130.9, 130.12, 128.25, 127.89, 127.17, 124.3, 113.2 (aromatic C, DMTr and nosyl), 86.7 (quaternary C, DMTr), 64.7,64.5 (CH_2O, CH_3O-N), 55.3 (OCH_3-DMTr, CH_2N), 21.3 (quaternary C).

HSQC (500MHz, $CDCl_3$): Correlation observed between δ H 6.7-8.33 ppm and δ C 113.2-158.6 (aromatic DMTr and nosyl), δ H 3.70, ppm and δ C 55.2 ppm (OCH_3, DMTr group), δ H 3.63 and δ C 64.7 (CH_2OH), δ H 3.52 and δ C64.5 (CH_3O-N), δ H 2.90-3.18 ppm and δ C 55.2 (CH_2-N).

ESI-TOF HRMS (ESI^+-TOF): *m/z* calc. for $[M+Na]^+$: 889.21 Da ; Found: 889.1586 Da.

2.3 Application of linker intermediate 3 in ON synthesis

Compound **3** serves as a versatile intermediate in the synthesis of ON-modifying building blocks. It was employed to generate two key functional units: a solid-support and a phosphoramidite building block, each designed for distinct purposes in ON modification.

- **Solid support:**

The solid-support was designed to be incorporated at the terminal position of ONs during solid-phase synthesis. By attaching the linker to a solid support, the ON sequence is efficiently synthesized in a stepwise manner. The terminal positioning of the linker ensures minimal interference with the overall ON sequence while providing a functional group for further chemical modification or conjugation.

- **Phosphoramidite Building Block:**

The phosphoramidite building block was developed for internal functionalization of ONs. This intermediate is strategically used to introduce functional groups at specific positions within an ON sequence, enabling the incorporation of modifications. The phosphoramidite linkage allows for efficient coupling during solid-phase synthesis, ensuring that the linker can be placed at a precise internal location in the sequence.

Both applications of linker intermediate **3** demonstrate its utility in expanding the functional diversity of ONs, providing new opportunities for the design of custom-modified nucleic acids for therapeutic, diagnostic, and research applications.

2.3.1 Synthesis of solid support for 3′-ON synthesis from DMTr-nosyl protected pentaerythritol, Compound **5**

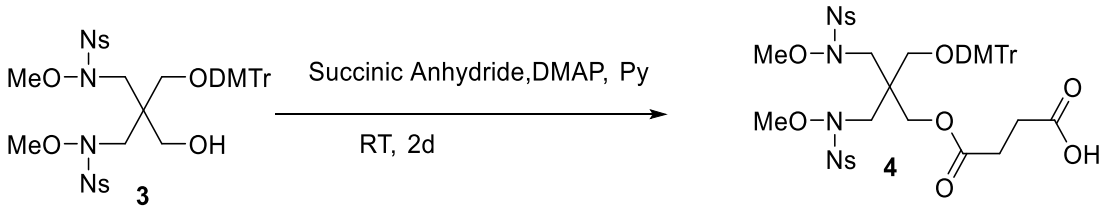

Scheme 7 Attaching compound **3** to succinic acid

As shown in scheme 7, for the synthesis of compound **4**, compound **2** (30 mg, 0.034 mmol) was dissolved in dry pyridine (1 ml), followed by the addition of succinic anhydride (4.8 mg, 0.048 mmol) and 2 grains of DMAP. The reaction mixture was stirred at room temperature for 48 h. During the reaction, the progress was monitored by TLC.

Once the reaction was finished, the solvent was evaporated, leaving behind the crude product. Purification was carried out using silica gel chromatography with a solvent system of 10:90 MeOH(10%): DCM (90%). The final yield of purified products was 65%, and ESI-TOF HRMS confirmed the formation of compound **4** in negative mode, where observed $[M-1]^{-1}$ ion appeared at 965.2348 Da, closely matching the expected exact mass 966.23 Da.

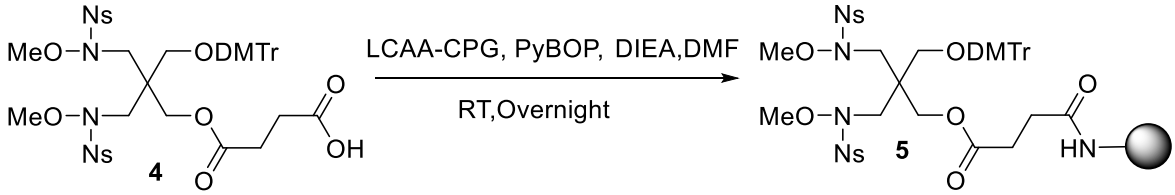

Scheme 8 Synthesis of functionalized solid support **5**

Following this step, the synthesized product was coupled to a solid support, Scheme 8. For this purpose, LCAA-CpG (113.8 mg, 2 eq.) was pretreated by soaking and washing with a mixture of TEA and methanol in a 1:9 (*v/v*) ratio, followed by drying under vacuum to remove any residual solvent. The dried solid was then suspended in dry DMF and treated with succinate **4** (21.8 mg, 22.56 µmol), PyBOP (12.94 mg, 24.85 µmol), and

DIPEA (7,84 µL, 45.12 µmol). The reaction was kept under continuous shaking overnight at room temperature.

Following the reaction, the suspension was filtered and the solid was rinsed with DMF and DCM to remove any unreacted reagents. The functionalized support was subjected to acetylation by suspending it in a 1:1 ratio of Cap A (acetic anhydride) to Cap B (lutidine/1-methyl imidazole). The mixture was shaken for 1 h. Afterward, the acetylated solid support was filtered, washed with THF and DCM to remove any excess reagents, and then dried under vacuum. A small sample (2.8 mg) of the acetylated solid support was exposed to 3% trichloroacetic acid (TCA) solution in DCM using the DMTr-cation assay to determine the loading capacity. The result indicated a loading capacity of 53 µmol. g^{-1}.

2.3.1.1 Synthesis of T4 ON-Compound **7**

The ON was synthesized through the process shown in Scheme 9, on a 1.0 µmol scale using an automated DNA/RNA synthesizer. The functionalized solid support **5** was loaded into the synthesizer, and synthesis was performed using commercial dT/CE phosphoramidite building blocks. Each coupling cycle had a recycling time of 2 min. After the completion of the ON synthesis, the solid support was placed under vacuum overnight to remove all solvents.

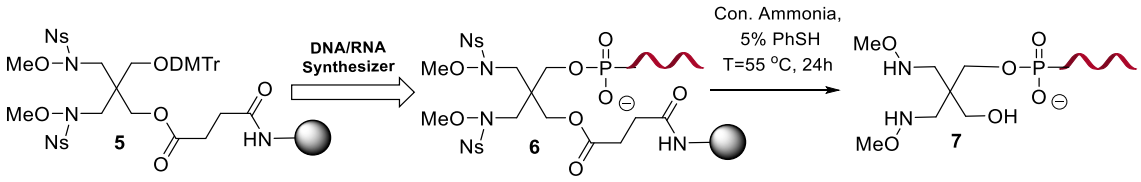

Scheme 9 Synthesis of terminal-modified ON T4 **7**

Following this, for the synthesis of terminal-modified ON T4, Scheme 9, the solid support-bound ON was treated with 250 µL of concentrated ammonium hydroxide and 12.5 µL of thiophenol. The reaction mixture was incubated at 55℃ for 24 h, allowing for the cleavage of the ON from the solid support and the removal of the nosyl group. After 24 h, the solvents were evaporated, and the resulting product was dissolved in MQ water for further purification.

RP-HPLC was used to purify the synthesized ON products. The separation was carried out on a Hypersil ODS C18 column (250× 4.6 mm, 5 μm), using a binary solvent system:

Solvent A: 50 mM triethylammonium acetate (TEAA) buffer (aqueous phase)

Solvent B: 1:1 (v/v) mixture of acetonitrile and 50mM TEAA (organic phase)

The gradient program was as follows:

t/min	Solvent A	Solvent B
0	90	10
20	30	70
25	30	70
30	90	10
35	90	10

The flow rate was maintained at 1.0 mL/min throughout the 35-min run. Elution was monitored by UV-Vis absorbance at 260 nm, and fractions at RT=14 min, showing a sharp peak, containing the target ON, were collected. The solvent was then removed using freeze-drying. The ESI-TOF HRMS results confirmed the formation of the desired product with the exact mass of 1410.31. The molecular ions were observed at 1421.3049 Da for formaldehyde adduct and 1435.3282 Da for acetaldehyde adduct.

2.3.2 Synthesis of intrachain-modified ON **11** from DMTr-nosyl protected Pentaerythritol

2.3.2.1 Synthesis of phosphoramidite for interchain-modified ON from DMTr-Nosyl protected Pentaerythritol - Compound **8**

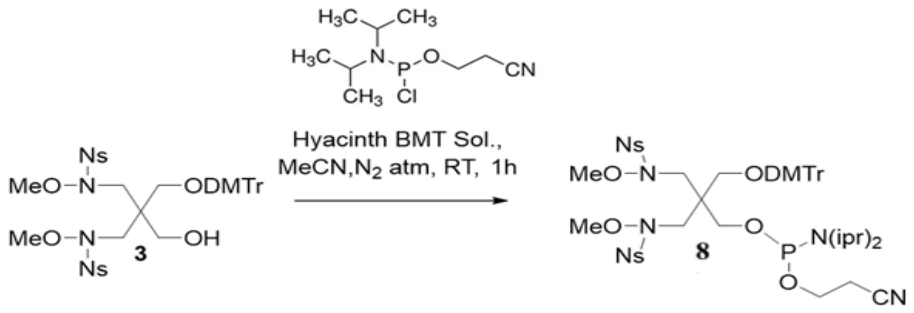

Scheme 10 Synthesis of Phosphoramidite **8**

To synthesize phosphoramidite **8**, scheme 10, 85.0 mg of compound **3** (0.1 mmol, 1 eq) was dissolved in 2.5 mL of MeCN under a nitrogen atmosphere. 42 µL of DIPEA (0.24 mmol, 2.4 eq) was added, followed by 27 µL (0.12 mmol, 1.2 eq) of *N, N*-diisopropylphosphoramidite. Stirring was continued under nitrogen 1 h. After the reaction was completed, the solvent was evaporated. The crude product was purified by silica gel chromatography using a mixture of DCM: MeOH: TEA (79.5:10:0.5(*v*/*v*/*v*)) as a solvent. After purification, 98 mg (0.092 mmol) of the product was obtained, yielding 92%.

^{1}H NMR (500 MHz, $CDCl_3$): δ 8.33 (4H, d , J = 9.0Hz, aromatic H, ortho to NO_2), 7.96 (4H, d, J = 9.0Hz, aromatic H, meta to NO_2), 7.12-7.25 (9H, aromatic H, DMTr group), 6.7 (4H, aromatic H, DMTr group), 4.89 (2H, CH_2-O-P), 3.70 (6H, 2×OCH_3, DMTr group), 3.56 (6H, 2×CH_3O-N), 3.37 (2H, CH_2ODMTr), 3.18 (2H, CH_2-CH_2-CN), 2.62 (8H, Overlapping signals including 2×CH_2N (4H), CH_2CN(2H)), 1.05-1.20 (CH_3, diisopropylamino group).

Note: The integration values in the region of δ 2.62 ppm and δ 1.05-1.20 ppm appear over-integrated compared to the expected number of protons in the structure. This over-integration is attributed to the presence of residual TEA, which is used as a component of the purification solvent system (DCM:MeOH: TEA). TEA is known to exhibit ^{1}H

NMR signals at approximately δ 2.62 ppm (CH_2) and δ 1.21ppm (CH_3) in $CDCl_3$, which overlap with the synthesized product methylene and methyl signals, respectively. Despite this, all characteristic proton signals of the target phosphoramidite compound **8** were identified and matched to the structure, confirming its successful synthesis.

COSY NMR (500 MHz, $CDCl_3$): COSY cross-peaks confirmed vicinal coupling between CH_2 protons in the -CH_2-CH_2-CN (3.17↔ 2.62 ppm), CH_2-O-DMTr, and CH_2-N groups. Aromatic correlations were consistent with the DMTr and nosyl substitution patterns.

^{13}C NMR (126 MHz, $CDCl_3$): δ 158.6, 151.1, 144.1, 138.57, 135.3, 130.9, 130.12, 128.25, 127.89, 127.17, 124.3, 113.2 (aromatic C, DMTr and nosyl), 86.7 (quaternary C, DMTr), 64.7,64.5 (CH_2O, CH_3O-N), 55.3 (OCH_3-DMTr, CH_2N), 21.3 (quaternary C).

^{13}P NMR (126 MHz, $CDCl_3$): $\delta \approx +$ 147 ppm (P(III)).

HSQC (500MHz, $CDCl_3$): HSQC cross-peaks conformed one-bond ^{1}H-^{13}C correlations for CH_2-O-P (δ H 4.89 / δ C 64.4), CH_2-O-DMTr (δ H 3.37 / δ C 76.8), and CH_2-CH_2-CN (δ H 3.17 & 2.62 / δ C 46.0 & 43.0). OCH_3, DMTr groups corelated at δ H 3.37 / δ C 55.2. Aromatic correlations are also consistent with the DMTr and nosyl substitution patterns.

2.3.2.2 Incorporation of phosphoramidite **8** into hairpin

The incorporation of compound **8** was achieved in the ON 5'-GCCAGUGCUCGUUUUCGAGCXCUGGC-3', where X represents the position of the modification. The synthesis was performed in multiple steps using manual conjugation and an automated DNA/RNA synthesizer and manual post-synthetic modifications.

2.3.2.2-a Initial sequence assembly and manual conjugation-Compound **9**

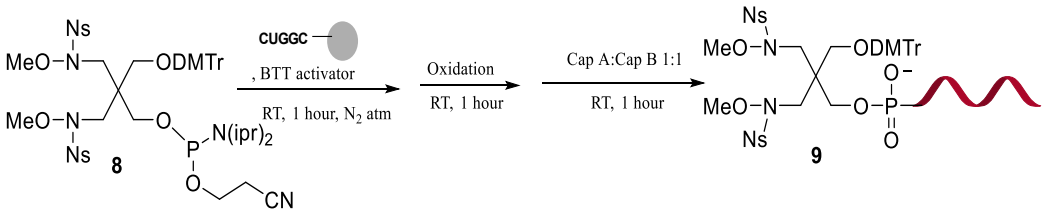

Scheme 11 Manual conjugation to the ON sequence

The synthesis as illustrated in Scheme 11, began with the preparation of short ON fragment 5'- GCUGGC-3', synthesized on a 5.0 µmol scale using standard phosphoramidite chemistry. Commercially available phosphoramidite building blocks and solid support were employed. Each coupling was carried out with a recycle time of 2 min. Upon completion, the solid support was washed with dry MeCN/DCM and placed under vacuum.

The 5'-modification was carried out manually by conjugation of compound **8** to the solid-support-bound ON under inert conditions. 47 mg (0.044 mmol) of compound **8** was dissolved in 200 µL of dry MeCN and added to the reaction vessel containing the ON support under nitrogen atmosphere. Subsequently, 225 µL (0.675 mmol) of 0.3 M BTT activator was added, and the mixture was stirred for 1 h at room temperature. Oxidation was performed by treating the support with 2.5 mL of 0.02 M I_2 (oxidizing agent) for 1 h. The support was then capped using a 1:1 mixture of Cap A and Cap B, followed by vacuum drying.

2.3.2.2-b Completion of hairpin structure and final deprotection-Compound **11**

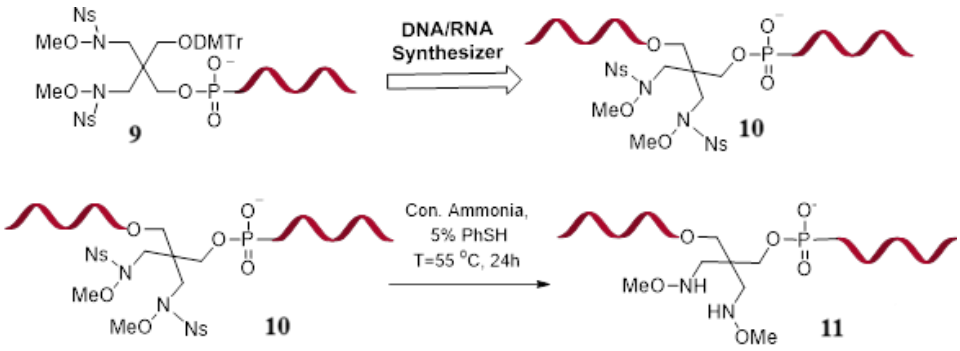

Scheme 12 Synthesis of hairpin structure and final deprotection 11

The remaining hairpin sequence was incorporated using compound **9**, which was loaded into the synthesizer. This synthesis, scheme 12, was conducted on a 1.0 µmol scale under standard conditions. Upon completion, the solid support was dried under vacuum overnight. Cleavage and deprotection were carried out by treating solid support with 1.0 mL of concentrated ammonium hydroxide and 50 µL of thiophenol. The reaction mixture was incubated at 55℃ for 24 h to enable cleavage from the solid support and complete removal of the nosyl protecting group. After the incubation period, the reaction mixture was evaporated to dryness, and the crude products were dissolved in MQ water for purification. Purification was performed by RP-HPLC on a Desc-clarity oligo-RP LC column, (250× 10 mm, 5µm). The following binary solvent system was used:

Solvent A: 50 mM triethylammonium acetate (TEAA) buffer (aqueous phase)

Solvent B: 1:1 (v/v) mixture of acetonitrile and 50mM TEAA (organic phase)

The gradient program was as follows:

t/min	Solvent A	Solvent B
0	90	10
20	50	50
25	50	50
30	90	10
40	90	10

The flow rate was maintained at 3.0 mL/min, and elution was monitored at 260 nm using UV-Vis detector. Four major fractions were collected at RT=10, 14, 17, and 27 min, respectively. Freeze drying was used to remove solvents from the collected fractions. ESI-TOF HRMS was used to confirm the identity of the synthesized product. The fraction eluted at RT=17 min exhibited molecular ion m/z 2139.387 Da for $[M-4H]^{4-}$ (formaldehyde adduct) and m/z 2142.39 Da for $[M-4H]^{4-}$ (acetaldehyde adduct), confirming successful incorporation of the modified unit.

3 Results and discussions

3.1 Synthesis of mono-DMTr-protected pentaerythritol, compound 2

For synthesis of compound **2**, pentaerythritol was selected as the starting material. The synthesis began with the selective mono-protection of pentaerythritol using 4,4'-dimethoxytrityl chloride (DMTrCl) in pyridine/DMSO. Because all four hydroxyl groups in pentaerythritol are chemically identical, the reaction lacks inherent selectivity, often leading to a mixture of partially and fully substituted products. This was addressed through stoichiometric control and a strict purification process. A multi-step purification involving four silica gel chromatographies with optimized solvent systems allowed the separation of the desired mono-DMTr.

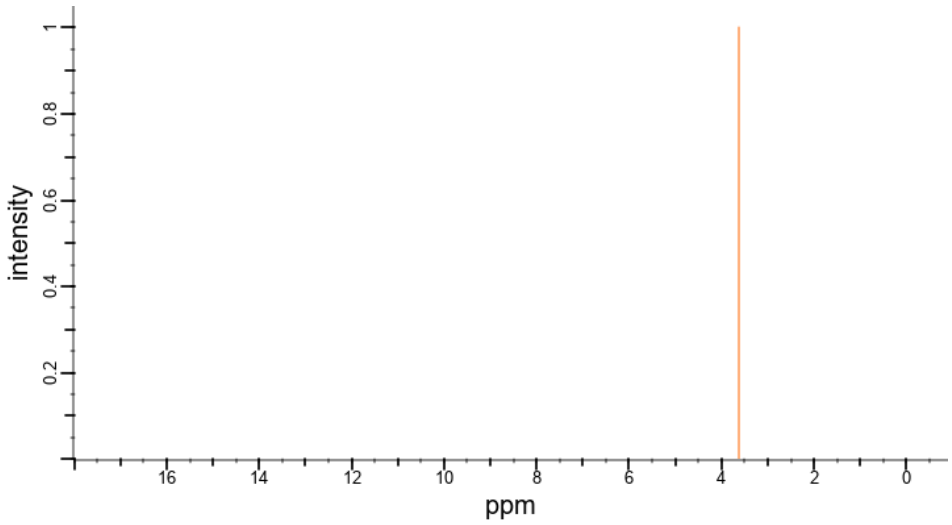

Figure 3 ^{1}H NMR of pentaerythritol

Structural characterization was consistent with the expected mono-substituted product. The ^{1}H NMR spectrum showed a more crowded spectrum compared to pentaerythritol (Figure 3). Aromatic peaks appear at δ 6.8-7.4 ppm corresponding to the DMTr group. A singlet at δ 3.76 ppm (OCH_3), δ 3.72 ppm for CH_2OH, and δ 3.13 ppm for the CH_2 group adjacent to DMTr moiety confirmed the presence of the DMTr group. ^{13}C NMR spectrum showed a quaternary DMTr carbon at δ 86.3 ppm and aromatic signals in the 126-158

ppm range. HSQC data confirmed correlations between the aromatic protons and their respective carbons, as well as OCH_3 and CH_2 signals. ESI-TOF HRMS supported the structural assignment, with observed masses for $[M+Na]^+$ and $[2M+Na]^+$ at 461.1571 Da and 899.3514 Da closely matching theoretical values. The isolated yield of compound **2** was 56%, which is reasonable given the complex purification required.

3.2 Synthesis of nosyl-protected intermediate, compound 3

Compound **2** was then used as a substrate for selective substitution of two of the remaining three hydroxy groups with nosyl-protected methoxyamine via the Mitsunobu reaction. The use of DIAD and triphenylphosphine as activating agents enabled nucleophilic substitution. Purification was performed via two successive gradient silica gel chromatographies. The final compound exhibited clear signals in all characterization methods. The ^1H NMR spectrum displayed two distinct aromatic systems: one for DMTr group (δ 6.8-7.4 ppm, 13H) and another for the nosyl groups (δ 8.33 and 7.96 ppm, 4H each, ortho and meta to NO_2). The methylene signals appeared between δ 2.90-3.63 ppm, consistent with CH_2N, CH_2O, and CH_2OH. Groups. The ^{13}C NMR spectrum confirmed the presence of DMTr and nosyl aromatic carbons, OCH_3 (δ 55 ppm), and methylene carbons. HSQC cross-peaks showed good correlation for all proton-carbon pairs, including CH_2-N and CH_2O functionalities. Notably, the quaternary carbon of DMTr group (δ 86.7) lacked correlation due to the absence of a directly attached proton. ESI-TOF HRMS confirmed molecular ion at m/z 889.1586 Da $[M+Na]^+$, matching the calculated values. The results confirmed successful installation of the nosyl-protected aminooxy groups onto the pentaerythritol core.

3.3 Dual application of compound 3: Toward solid-support and phosphoramidite building blocks

Compound **3** served as a versatile intermediate, enabling two downstream applications for ON modification. First, it was used to synthesize a solid-support-compatible building block, designed for conjugation at the terminal end of ONs during solid-phase synthesis. This involved the attachment of the molecules onto a controlled-pore glass (CPG) resin via an appropriate linker, enabling ON elongation from the modified position. Second, compound **3** was converted into a phosphoramidite derivative by coupling with 2-cyanoethyl *N, N*-diisopropylphosphoramidite under dry, inert conditions. The resulting phosphoramidite, confirmed via ^{1}H NMR and ^{31}P NMR, showed characteristic signals for the diisopropyl groups and ^{31}P resonance in $\approx$ 147 ppm region, indicating successful formation of the reactive phosphoramidite moiety.

These two products offer complementary strategies for ON engineering: One for terminal anchoring via solid supports and the other for internal modification through direct incorporation during ON synthesis. Both platforms enhance the versatility of ON-based drug delivery.

3.4 Challenges in the nosyl group removal

During the final deprotection step following ON synthesis, the removal of the nosyl group posed a significant challenge. Although conventional protocols using concentrated aqueous ammonia were expected to efficiently cleave the solid support linker and remove the nosyl group, initial attempts proved unsuccessful.

Three deprotection conditions were tested at room temperature:

a) 5% thiophenol and 5% DBU in DMSO,

b) 5% thiophenol in concentrated aqueous ammonia, and

c) 5% thiophenol with 5% potassium carbonate in DMSO

None of these conditions yielded complete removal of the nosyl protecting group. Ultimately, efficient deprotection was achieved only by applying elevated temperature. A mixture of 5% thiophenol in concentrated ammonia at 55℃ for 24 h resulted in successful cleavage of both the nosyl group and the ON from the solid support.

The product was isolated and confirmed by RP-HPLC and ESI-TOF HRMS to be of the expected composition and purity.

This outcome underscores the sensitivity of the nosyl cleavage to temperature and suggests that elevated thermal conditions are essential for complete deprotection in the context of sterically hindered or support-bound systems

4 Conclusion

In this work, a stepwise and versatile synthetic strategy was developed for the synthesis of a pentaerythritol-derived ON linker bearing both DMTr and nosyl-protected functionalities. The synthesis involved the selective mono-protection of pentaerythritol followed by dual aminooxy substitution using nosyl-protected methoxyamine. Rigorous purification and comprehensive characterization (^{1}H, ^{13}C, HSQC NMR, and ESI-TOF HRMS) confirmed the successful formation of the key intermediate.

Compound **3** was then utilized in two parallel applications: a solid support-bound ON modifier and a phosphoramidite building block suitable for internal ON decoration. This dual-pathway approach provides a flexible platform for the development of stimulus-responsive ON conjugates, particularly in the context of pH-responsive drug delivery systems. The modularity and compatibility of these synthetic tools pave the way for further biological evaluation and integration into targeted therapeutic strategies.

Additionally, challenges encountered during nosyl deprotection highlight the importance of optimizing reaction conditions, particularly temperature, for efficient cleavage. The successful removal of nosyl group emphasizes the need for tailored deprotection strategies in ON systems incorporating sterically demanding protecting groups.

5 Future Perspectives

Future work will focus on kinetic studies of the ligation reaction between the synthesized *N, N*-dimethoxy-aminal linker and various aldehydes, analogous to the work by Aho et al.,[33] who determined reaction rates and equilibrium constants in the formation of pH-responsive N-methoxy azolidine linker between peptide aldehydes and ONs. This would allow a better understanding of reaction dynamics and cleavability of the system under physiologically relevant conditions.

Additionally, the potential of this linker in sequence-specific aldehyde capture within double-stranded DNA structures will be explored, inspired by the work of Afari et al. [45] who incorporated N-methoxy-1,3-oxazinane (MOANA) nucleoside analogues into hairpin ON to mimic Watson-Crick base pairing with aromatic aldehydes. Incorporating the dimethoxy-aminal linker into similar DNA hairpins could enable responsive or dynamic base-pairing systems for applications in molecular recognition, diagnostics, or programmable drug delivery.

6 References

1. Ulrich, S., *Growing prospects of dynamic covalent chemistry in delivery applications.* Accounts of chemical research, 2019. **52**(2): p. 510-519.
2. Stuart, M.A.C., et al., *Emerging applications of stimuli-responsive polymer materials.* Nature materials, 2010. **9**(2): p. 101-113.
3. Hu, J., G. Zhang, and S. Liu, *Enzyme-responsive polymeric assemblies, nanoparticles and hydrogels.* Chemical Society Reviews, 2012. **41**(18): p. 5933-5949.
4. Qiao, Y., et al., *Stimuli‐responsive nanotherapeutics for precision drug delivery and cancer therapy.* Wiley Interdisciplinary Reviews: Nanomedicine and Nanobiotechnology, 2019. **11**(1): p. e1527.
5. Li, Y. and D. Maciel, *Smart nanocarriers for targeted and triggered drug delivery.* Advanced Functional Materials, 2019. **29**: p. 1807335.
6. Zhang, A., et al., *Recent advances in stimuli-responsive polymer systems for remotely controlled drug release.* Progress in Polymer Science, 2019. **99**: p. 101164.
7. Stuart, M.A.C., et al., *Emerging applications of stimuli-responsive polymer materials.* Nature Materials, 2010. **9**(2): p. 101–113.
8. Majumder, J. and T. Minko, *Multifunctional and stimuli-responsive nanocarriers for targeted therapeutic delivery.* Expert opinion on drug delivery, 2021. **18**(2): p. 205-227.
9. Fatima, M., et al., *Harnessing the Power of Stimuli‐Responsive Nanoparticles as an Effective Therapeutic Drug Delivery System.* Advanced Materials, 2024. **36**(24): p. 2312939.
10. Shinn, J., et al., *Smart pH-responsive nanomedicines for disease therapy.* Journal of Pharmaceutical Investigation, 2022. **52**(4): p. 427-441.
11. Schneider, L.A., et al., *Influence of pH on wound-healing: a new perspective for wound-therapy?* Archives of dermatological research, 2007. **298**(9): p. 413-420.
12. Behbahani, S.B., et al., *pH variation in medical implant biofilms: Causes, measurements, and its implications for antibiotic resistance.* Frontiers in Microbiology, 2022. **13**: p. 1028560.
13. Smith, C.I.E. and R. Zain, *Therapeutic Oligonucleotides: State of the Art.* Annual Review of Pharmacology and Toxicology, 2019. **59**: p. 605–630.
14. Sharma, V.K. and J.K. Watts, *Oligonucleotide therapeutics: chemistry, delivery and clinical progress.* Future Medicinal Chemistry, 2015. **7**(16): p. 2221–2242.
15. Hammond, S.M., G. Hazell, and F. Shabanpoor, *Delivery of oligonucleotide-based therapeutics: challenges and opportunities.* EMBO Molecular Medicine, 2021. **13**: p. e13243.
16. Hu, Q., et al., *DNA nanotechnology-enabled drug delivery systems.* Chemical Reviews, 2018. **119**(10): p. 6459–6506.
17. Mergny, J.L. and D. Sen, *DNA quadruple helices in nanotechnology.* Chemical Reviews, 2019. **119**(10): p. 6290–6325.
18. Thakur, S., et al., *A perspective on oligonucleotide therapy: Approaches to patient customization.* Frontiers in Pharmacology, 2022. **13**: p. 1006304.
19. Lundin, K.E., O. Gissberg, and C.I.E. Smith, *Oligonucleotide therapies: the past and the present.* Human Gene Therapy, 2015. **26**(8): p. 475–485.

20. Lehn, J.-M. *Supramolecular Chemistry and Self-Organisation*. in *Supramolecular Chemistry and Self-Organisation*. 2009.
21. Rowan, S.J., et al., *Dynamic covalent chemistry.* Angewandte Chemie International Edition, 2002. **41**(6): p. 898-952.
22. Corbett, P.T., et al., *Dynamic combinatorial chemistry.* Chemical reviews, 2006. **106**(9): p. 3652-3711.
23. Bae, Y.H. and K. Park, *Targeted drug delivery to tumors: myths, reality and possibility*. 2011, Elsevier. p. 198-205.
24. Qiao, Y., et al., *Stimuli‐responsive nanotherapeutics for precision drug delivery and cancer therapy.* WIREs Nanomedicine and Nanobiotechnology, 2018. **11**: p. e1527.
25. Kloxin, A.M., et al., *Photodegradable hydrogels for dynamic tuning of physical and chemical properties.* Science, 2009. **324**(5923): p. 59-63.
26. DeForest, C.A. and K.S. Anseth, *Cytocompatible click-based hydrogels with dynamically tunable properties through orthogonal photoconjugation and photocleavage reactions.* Nature Chemistry, 2011. **3**(12): p. 925-931.
27. Jin, Y., et al., *Recent advances in dynamic covalent chemistry.* Chemical Society Reviews, 2013. **42**(16): p. 6634-6654.
28. Kölmel, D.K. and E.T. Kool, *Oximes and hydrazones in bioconjugation: mechanism and catalysis.* Chemical reviews, 2017. **117**(15): p. 10358-10376.
29. Bauhuber, S., et al., *Delivery of nucleic acids via disulfide‐based carrier systems.* Advanced materials, 2009. **21**(32‐33): p. 3286-3306.
30. Debiais, M., J.-J. Vasseur, and M. Smietana, *Applications of the Reversible Boronic Acids/Boronate Switch to Nucleic Acids.* The Chemical Record, 2022. **22**: p. e202200085.
31. Afari, M.N.K. and T. Lönnberg, *Base‐Filling in Double‐Helical Nucleic Acids.* ChemistryOpen, 2024. **13**(9): p. e202400088.
32. Afari, M.N.K., et al., *The Impact of Secondary Structure on the Base-Filling of N-Methoxy-1,3-Oxazinane (MOANA) and N-Methoxy-1,3-Oxazolidine Glycol Nucleic Acid (MOGNA) Oligonucleotides.* ChemBioChem, 2025. **26**(1): p. e202400666.
33. Aho, A., et al., *Conjugation of oligonucleotides to peptide aldehydes via a Ph-responsive N-methoxyoxazolidine linker.* Organic Letters, 2020. **22**(17): p. 6714-6718.
34. Aho, A., et al., *Expanding the scope of the cleavable N-(methoxy) oxazolidine linker for the synthesis of oligonucleotide conjugates.* Molecules, 2021. **26**(2): p. 490.
35. Aho, A., et al., *DNA‐Templated Formation and N, O‐Transacetalization of N‐Methoxyoxazolidines.* European Journal of Organic Chemistry, 2022. **2022**(31): p. e202200583.
36. Aho, A. and P. Virta, *Assembly of split aptamers by dynamic pH-responsive covalent ligation.* Chemical Communications, 2023. **59**(38): p. 5689-5692.
37. Buchs, B., et al., *Reversible aminal formation: Controlling the evaporation of bioactive volatiles by dynamic combinatorial/covalent chemistry*. 2011, Wiley Online Library.
38. Wang, Q.Y., et al., *Aminal‐linked porphyrinic covalent organic framework for rapid photocatalytic decontamination of mustard‐gas simulant.* Angewandte Chemie, 2022. **134**(32): p. e202207130.
39. Jiang, S.-Y., et al., *Aminal-linked covalent organic frameworks through condensation of secondary amine with aldehyde.* Journal of the American Chemical Society, 2019. **141**(38): p. 14981-14986.

40. Li, X. and D.R. Liu, *DNA‐templated organic synthesis: nature's strategy for controlling chemical reactivity applied to synthetic molecules.* Angewandte Chemie International Edition, 2004. **43**(37): p. 4848-4870.
41. Di Pisa, M. and O. Seitz, *Nucleic acid templated reactions for chemical biology.* ChemMedChem, 2017. **12**(12): p. 872-882.
42. Hickman, D.T., N. Sreenivasachary, and J.M. Lehn, *Synthesis of components for the generation of constitutional dynamic analogues of nucleic acids.* Helvetica Chimica Acta, 2008. **91**(1): p. 1-20.
43. Heemstra, J.M. and D.R. Liu, *Templated synthesis of peptide nucleic acids via sequence-selective base-filling reactions.* Journal of the American Chemical Society, 2009. **131**(32): p. 11347-11349.
44. Afari, M.N., P. Virta, and T. Lönnberg, *N-Methoxy-1, 3-oxazinane nucleic acids (MOANAs)–a configurationally flexible backbone modification allows post-synthetic incorporation of base moieties.* Organic & Biomolecular Chemistry, 2022. **20**(17): p. 3480-3485.
45. Afari, M.N., et al., *Watson‐Crick Base Pairing of N‐Methoxy‐1, 3‐Oxazinane (MOANA) Nucleoside Analogues within Double‐Helical DNA.* ChemistryOpen, 2023. **12**(7): p. e202300085.

7 Appendices

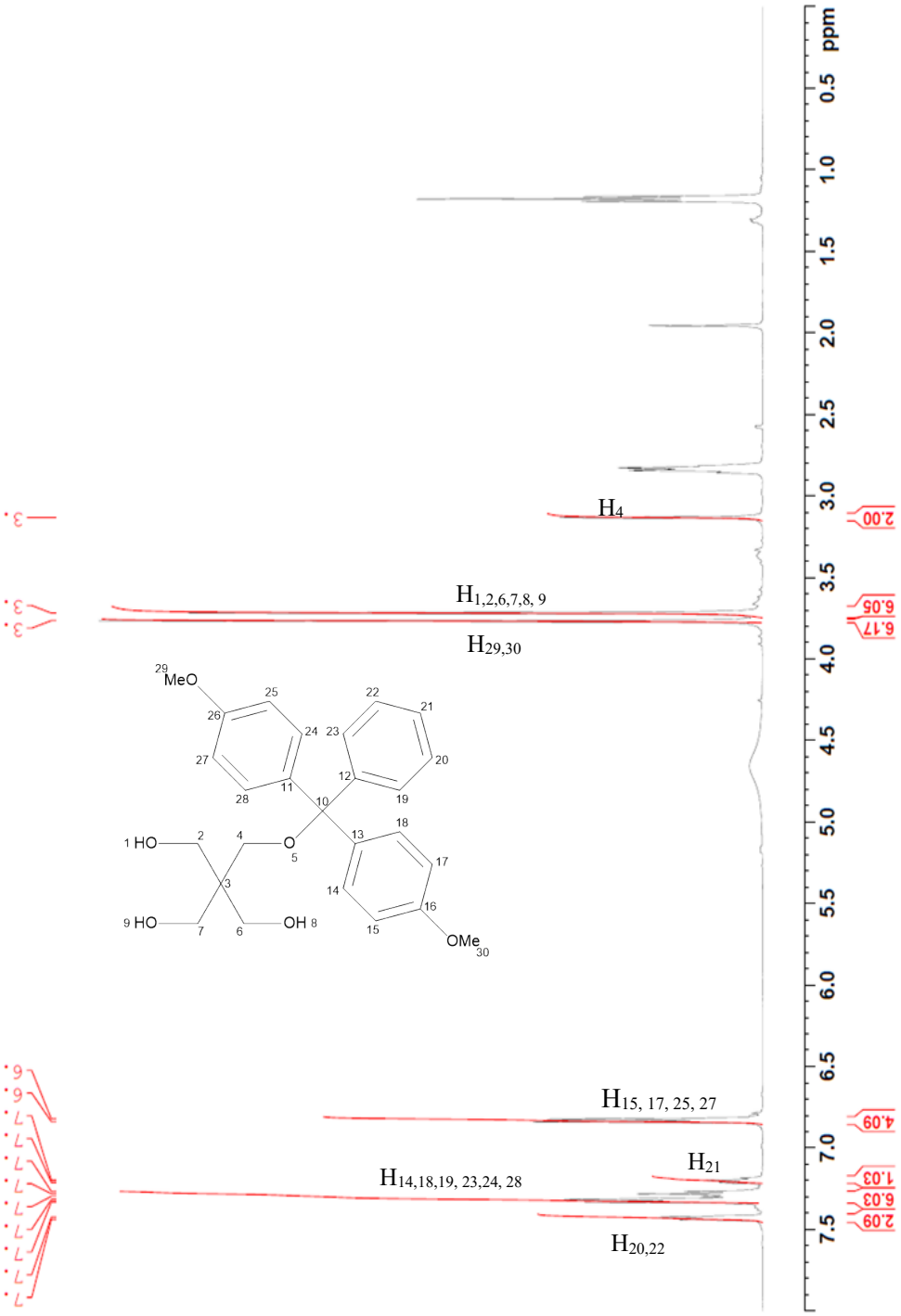

Figure 4 ^{1}H NMR spectrum of Compound **2**

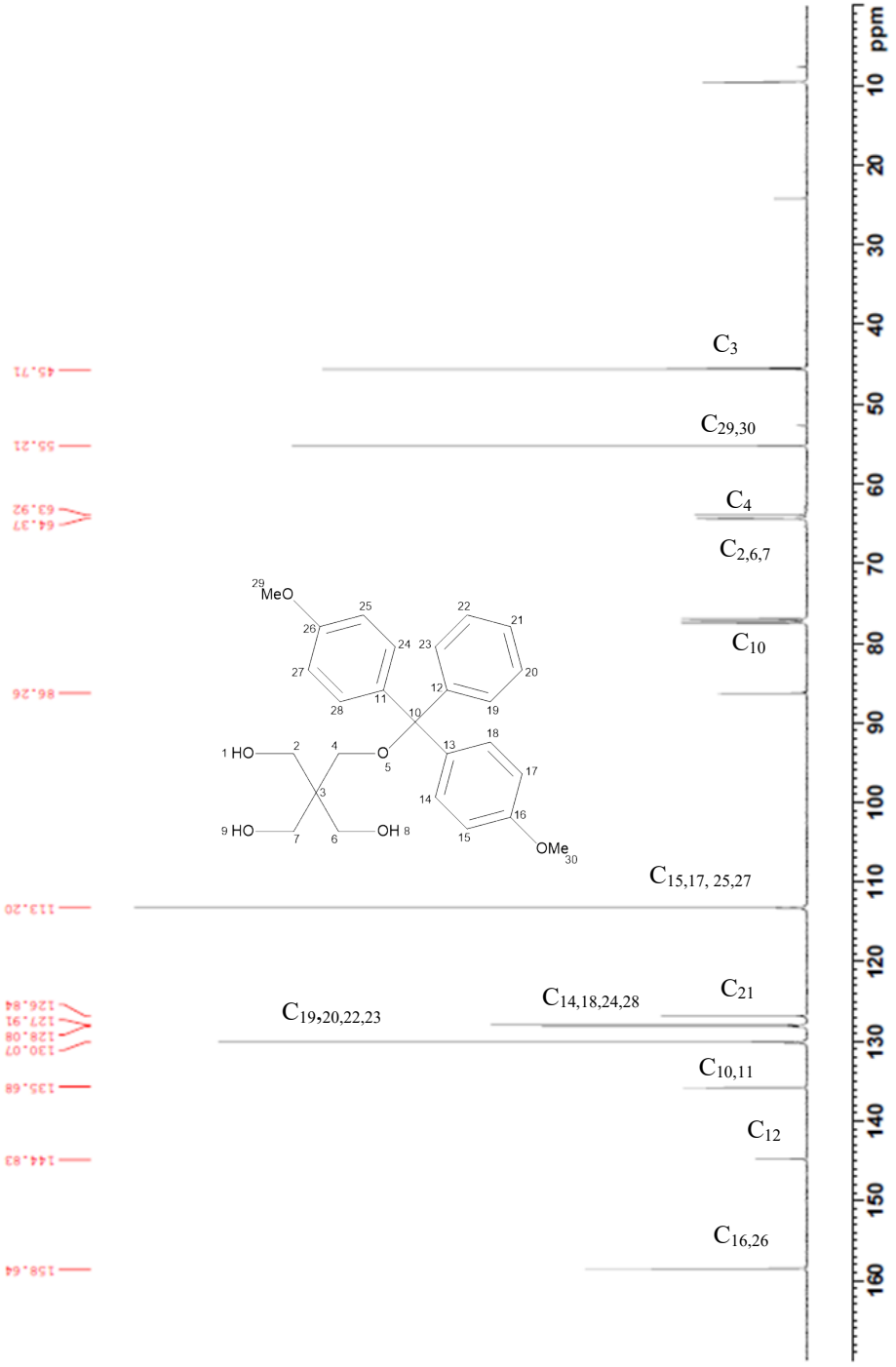

Figure 5 ^{13}C NMR of spectrum of compound **2**

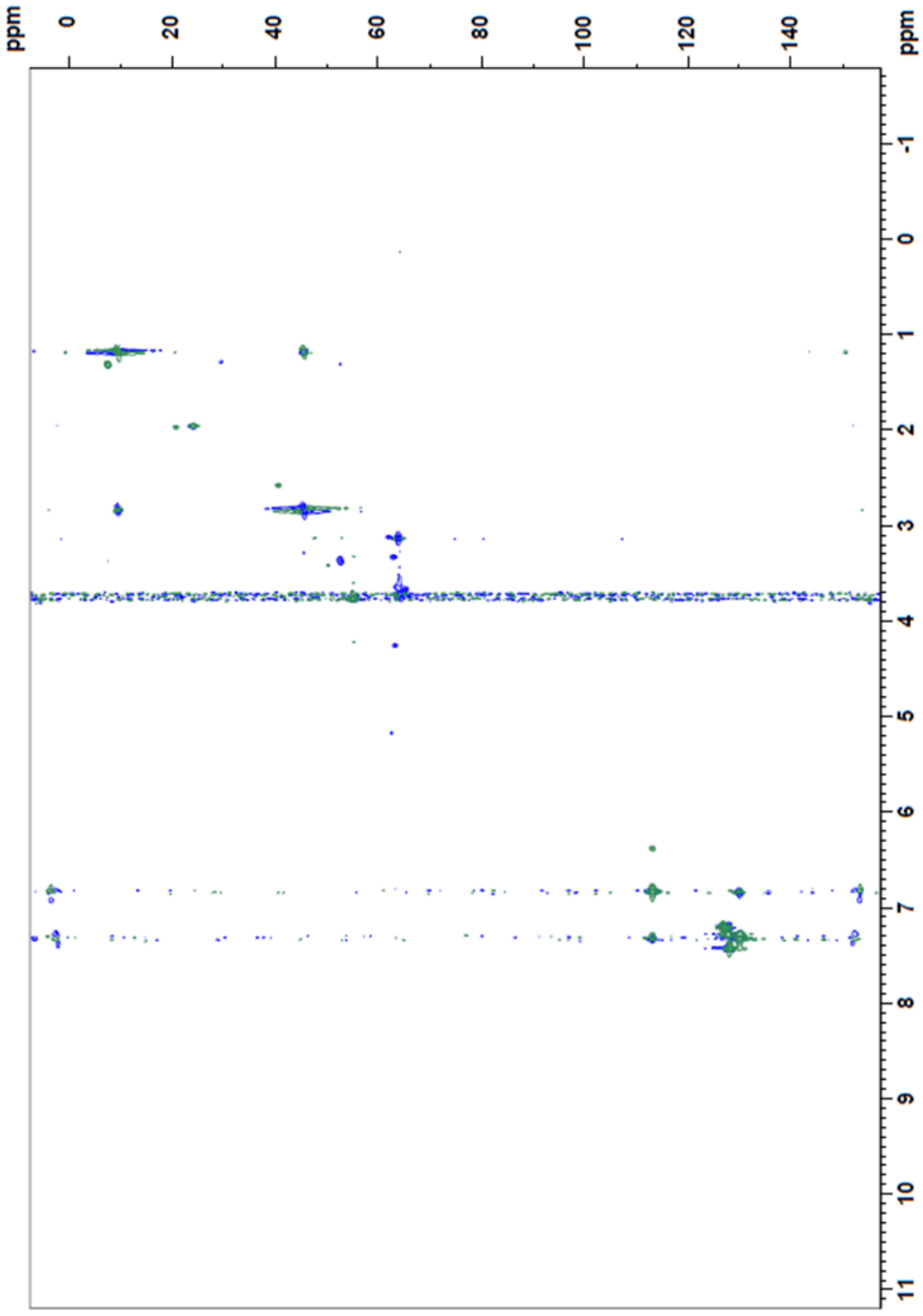

Figure 6 HSQC spectrum of compound **2**

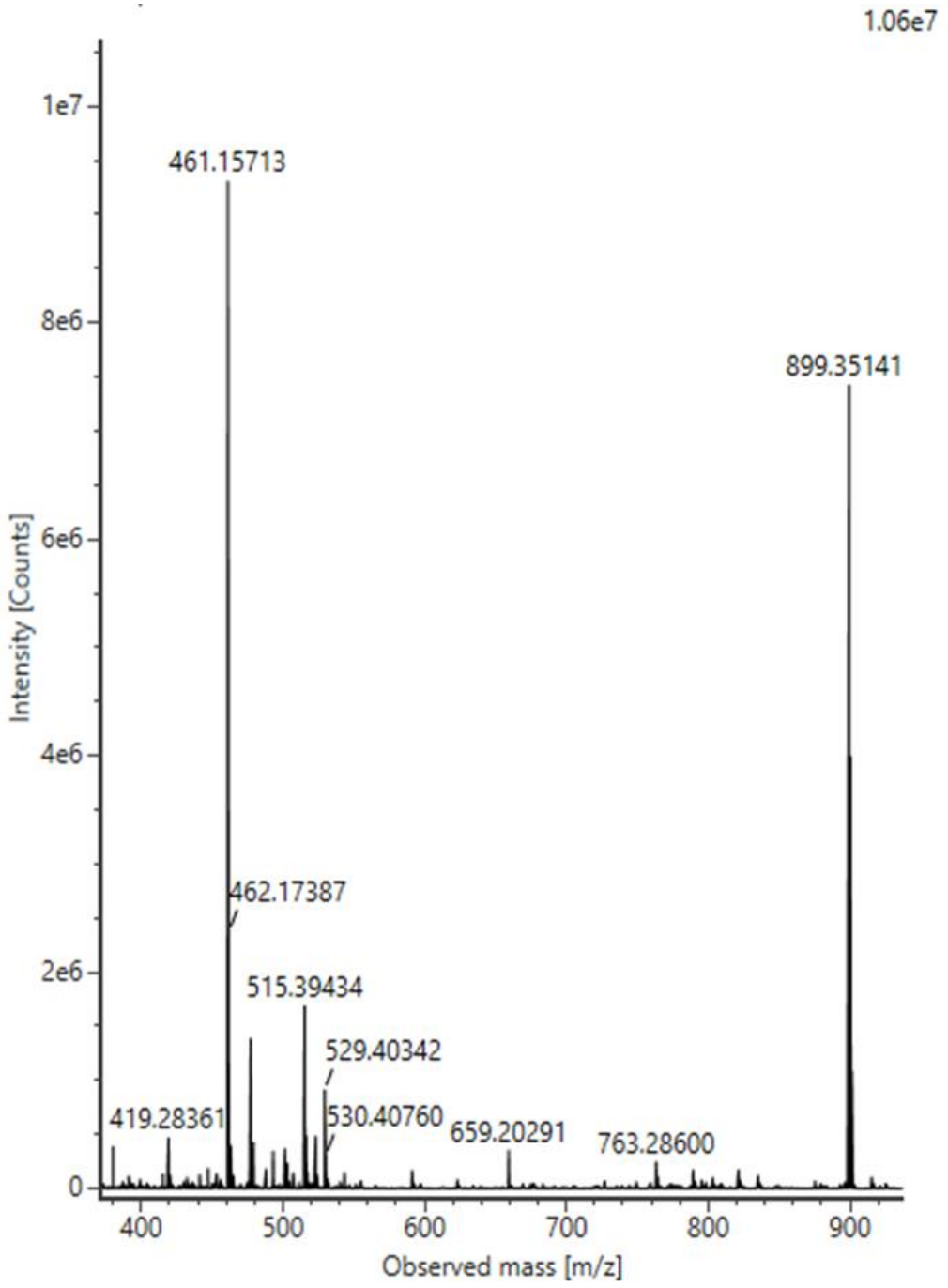

Figure 7 ESI-TOF HRMS spectrum of compound **2**, m/z :461.1571 Da for $[M+Na]^+$;

m/z :899.3514 Da for $[2M+Na]^+$

The spectrum quality enhanced using AI-based image processing

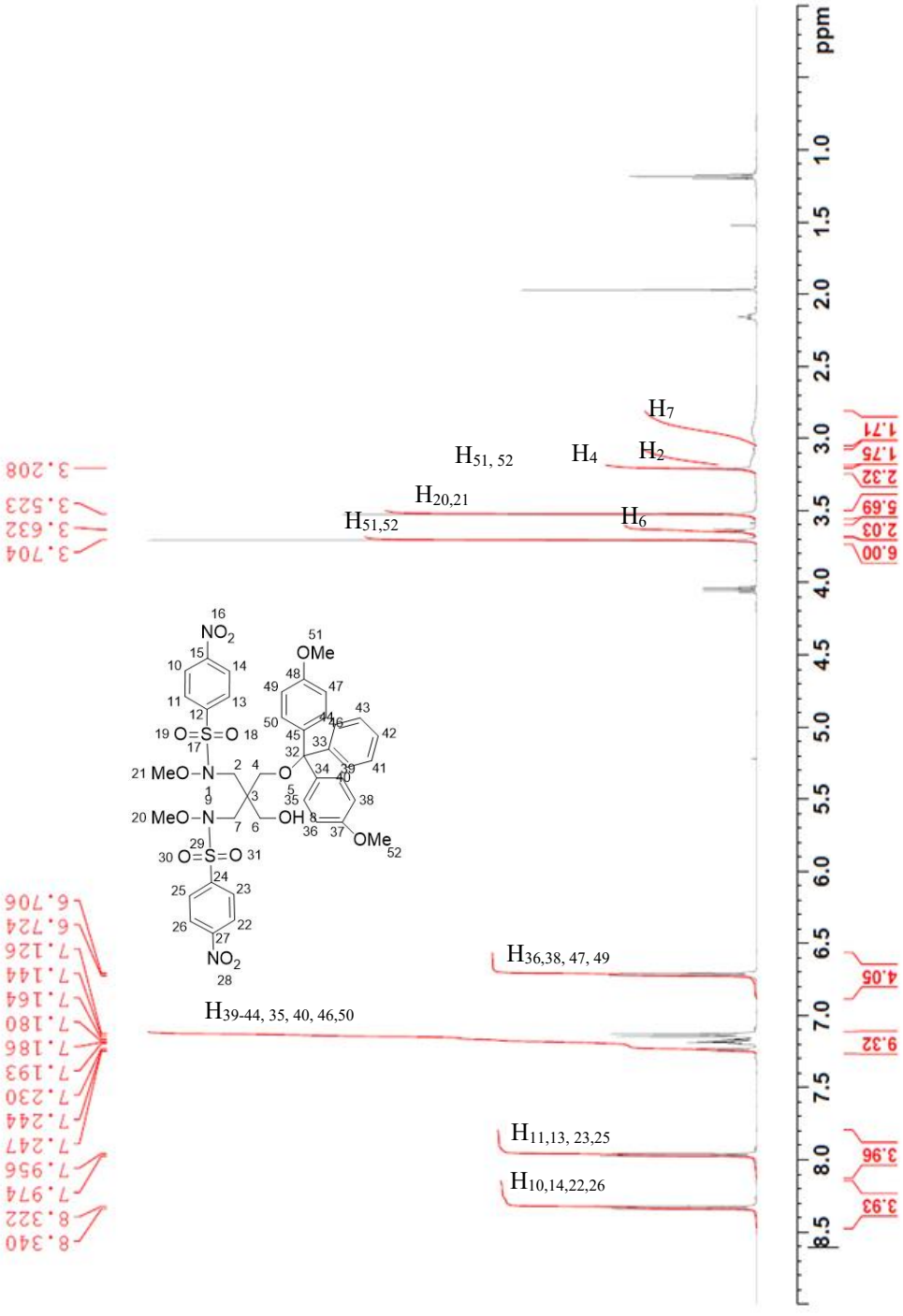

Figure 8 ^{1}H NMR of spectrum of compound **3**

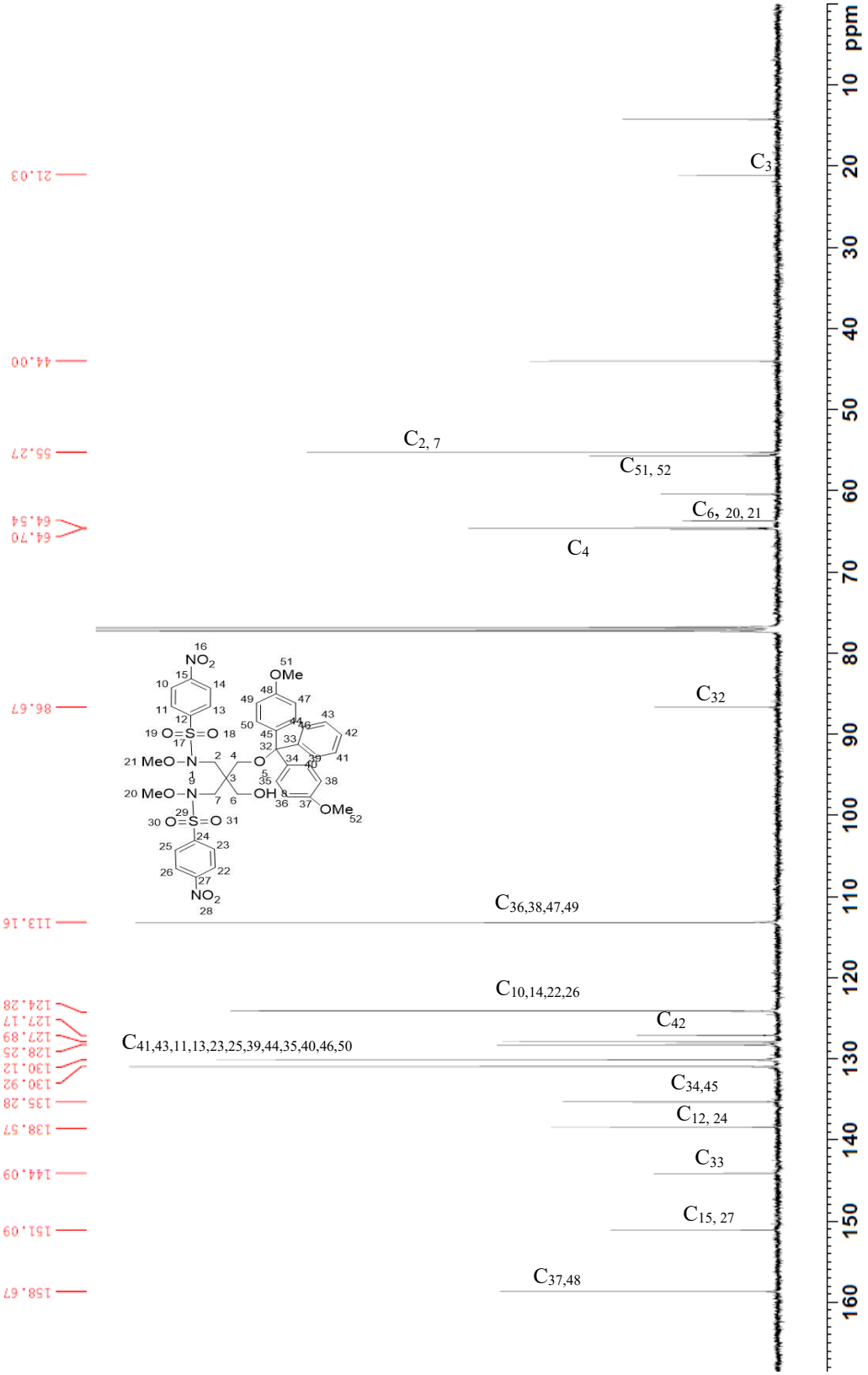

Figure 9 ^{13}C NMR spectrum of compound **3**

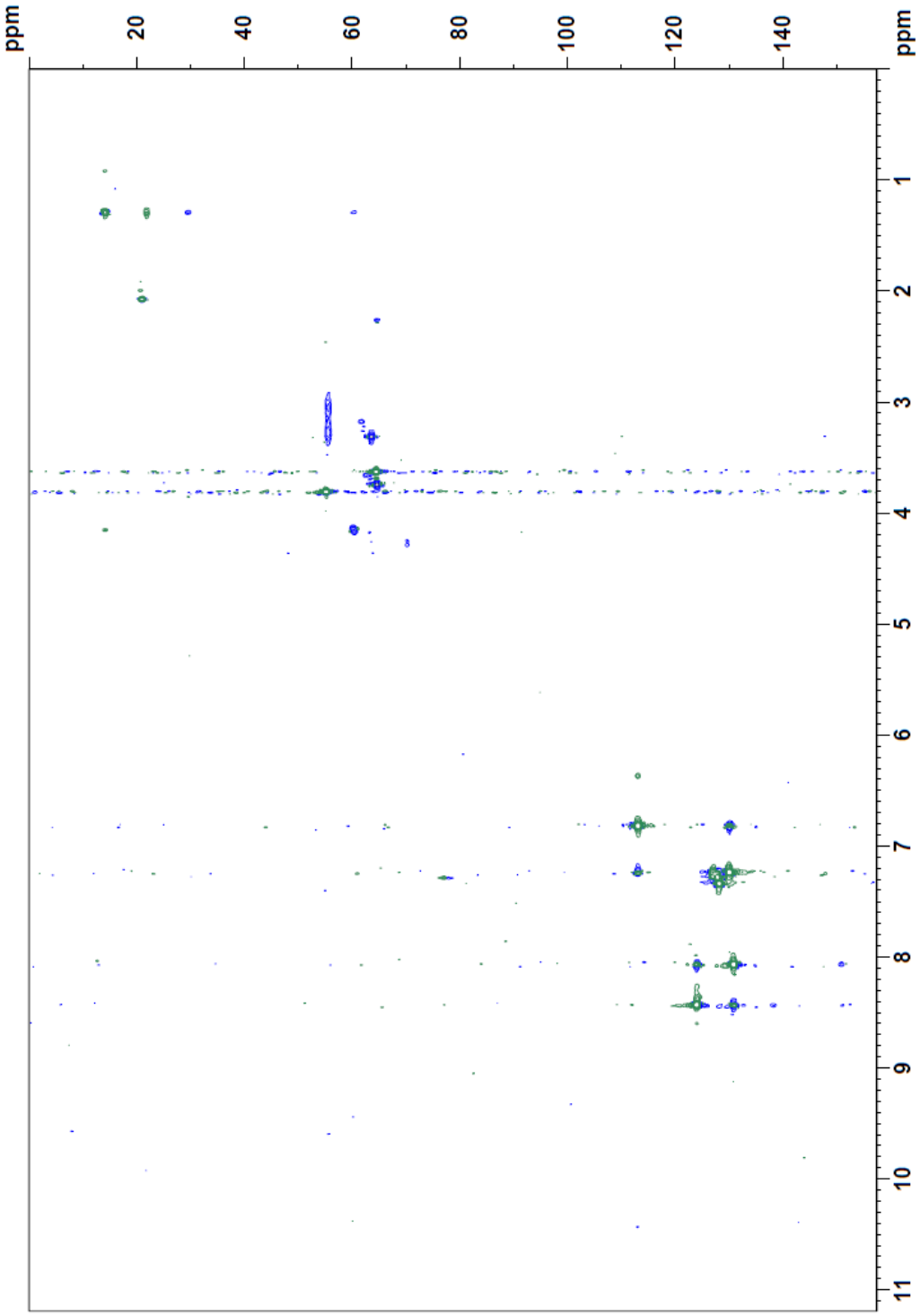

Figure 10 HSQC spectrum of compound **3**

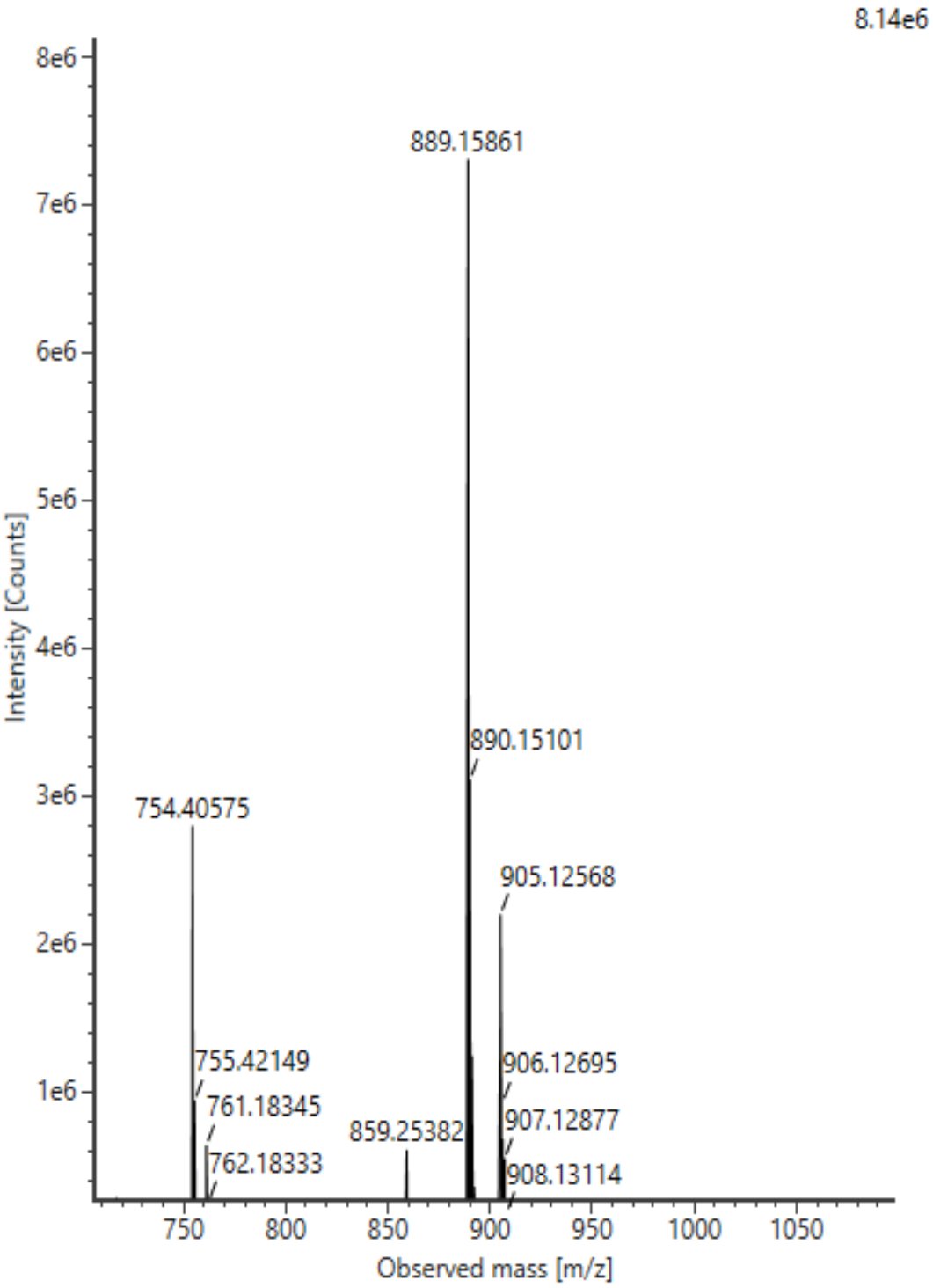

Figure 11 ESI-TOF HRMS spectrum of compound **3**, m/z : 889.1586 Da for $[M+Na]^+$

The spectrum quality enhanced using AI-based image processing

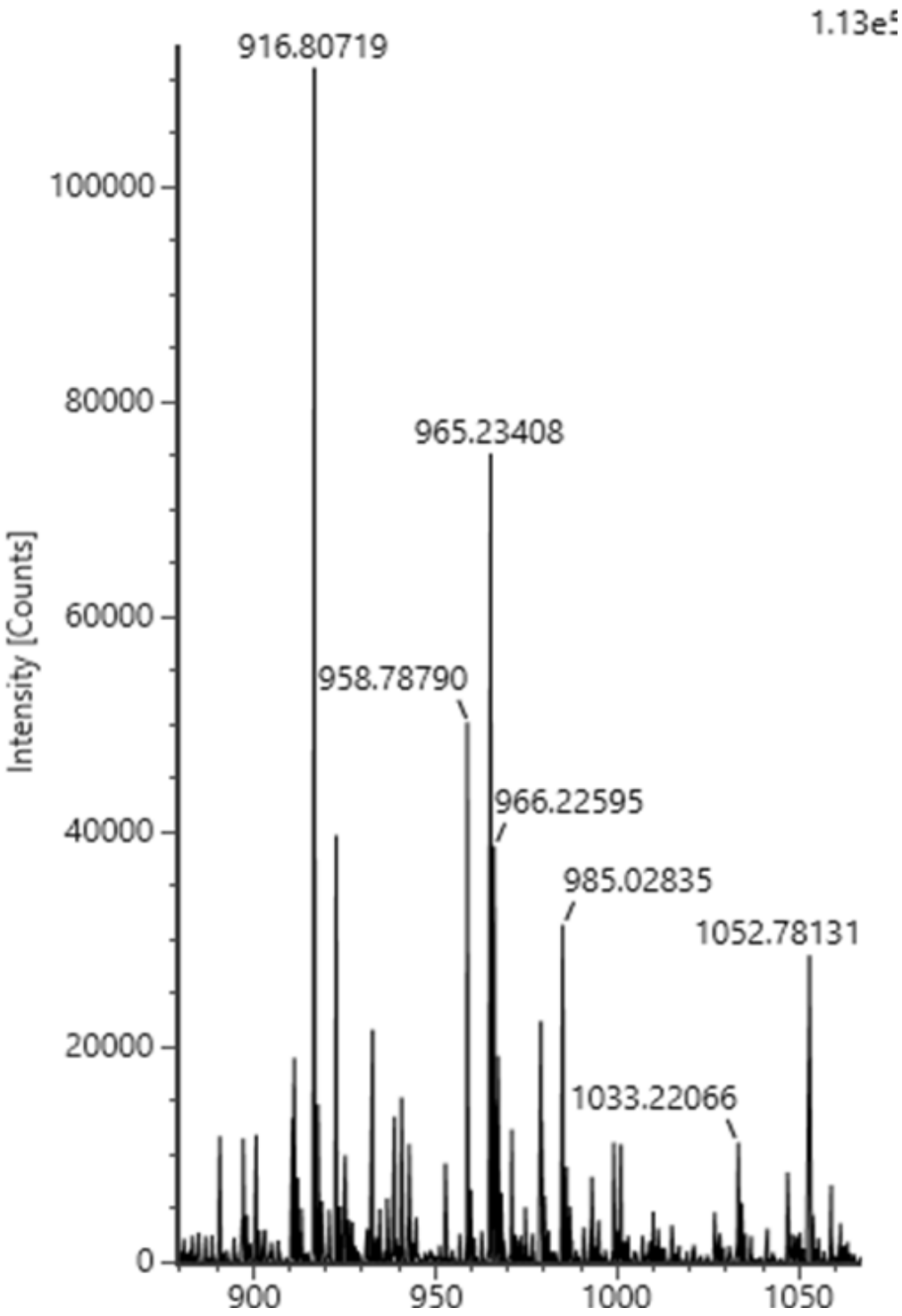

Figure 12 ESI-TOF HRMS of compound **4**, m/z: 966.2259 Da for $[M-1]^{-1}$

The spectrum quality enhanced using AI-based image processing

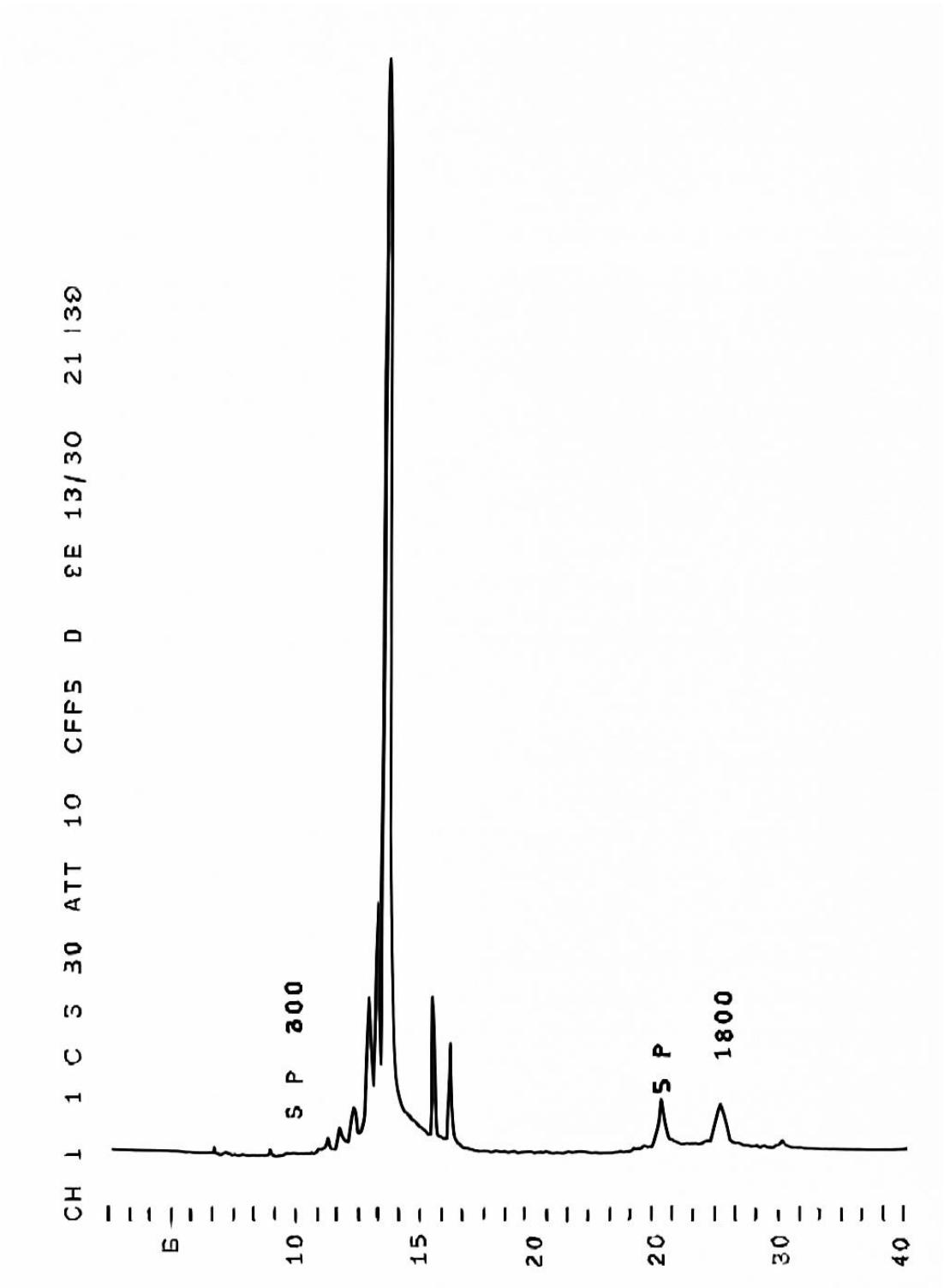

Figure 13 HPLC Chromatogram of the terminal-modified ON T4 synthesis reaction mixture after ammonolysis

The chromatogram enhanced using AI-based image processing

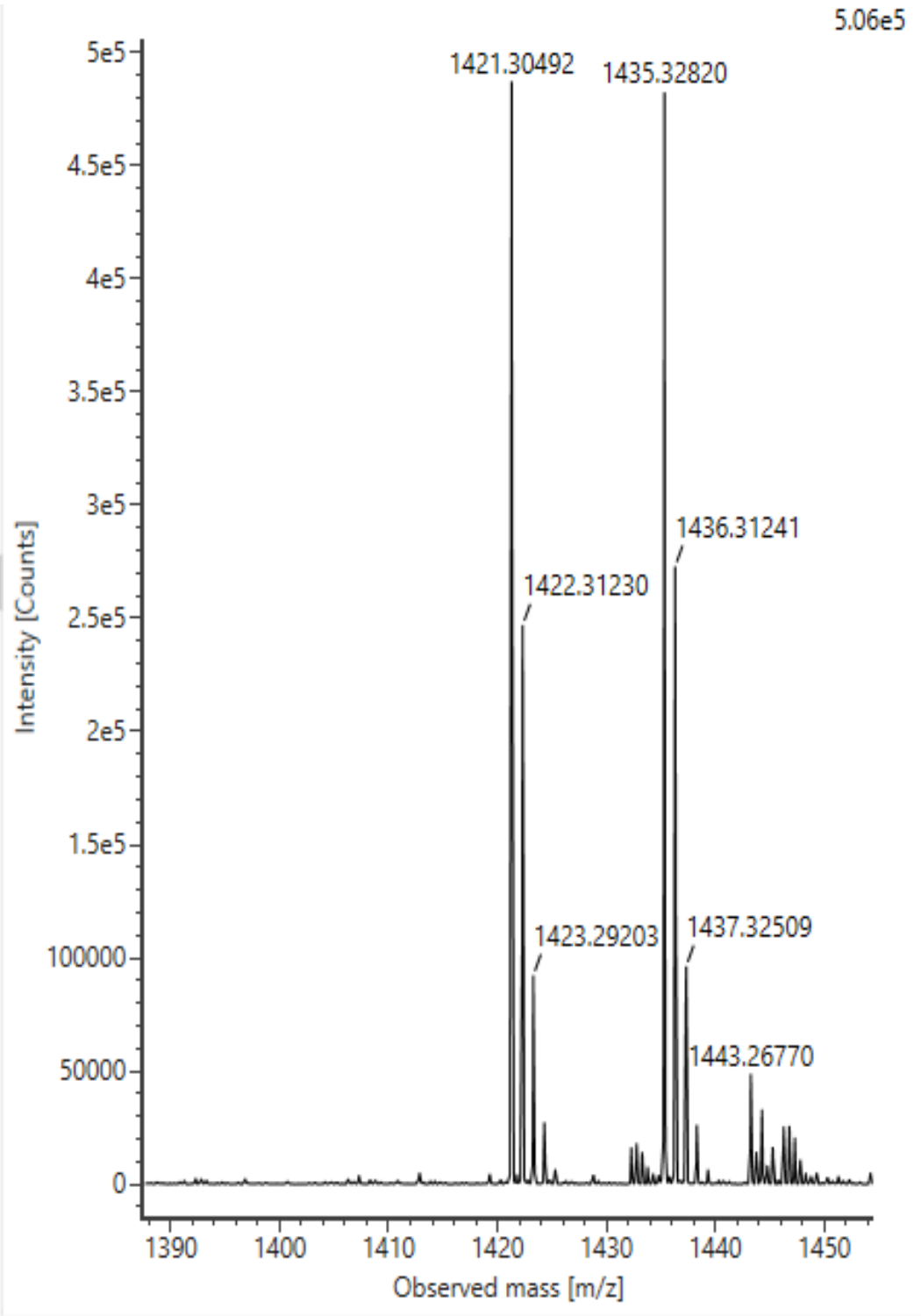

Figure 14 ESI-TOF HRMS of compound **7**, m/z : 1421.3049 Da for formaldehyde adduct m/z : 1435.3282 Da for acetaldehyde adduct

The spectrum quality enhanced using AI-based image processing

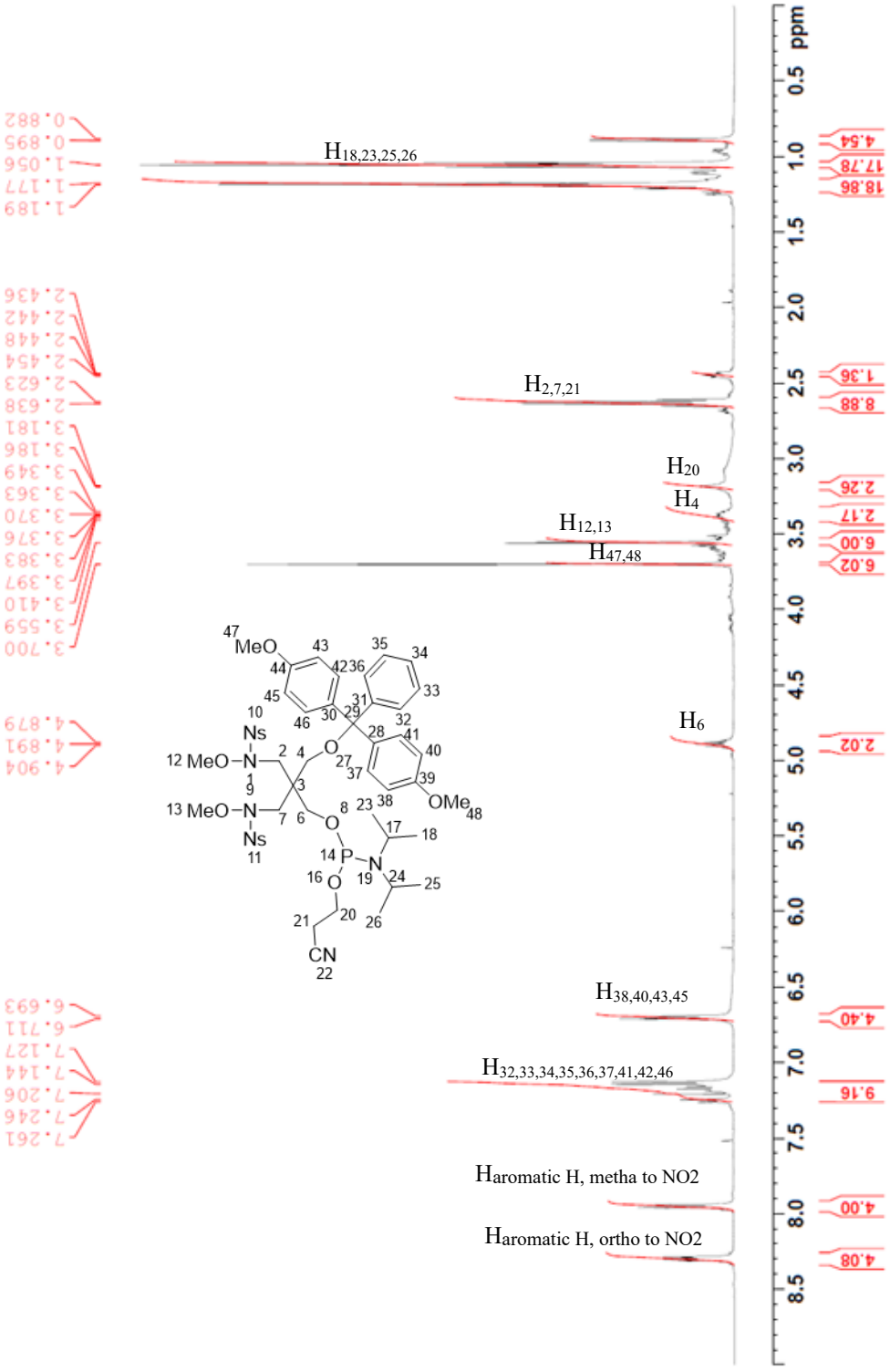

Figure 15 ^{1}H NMR spectrum of phosphoramidite **8**

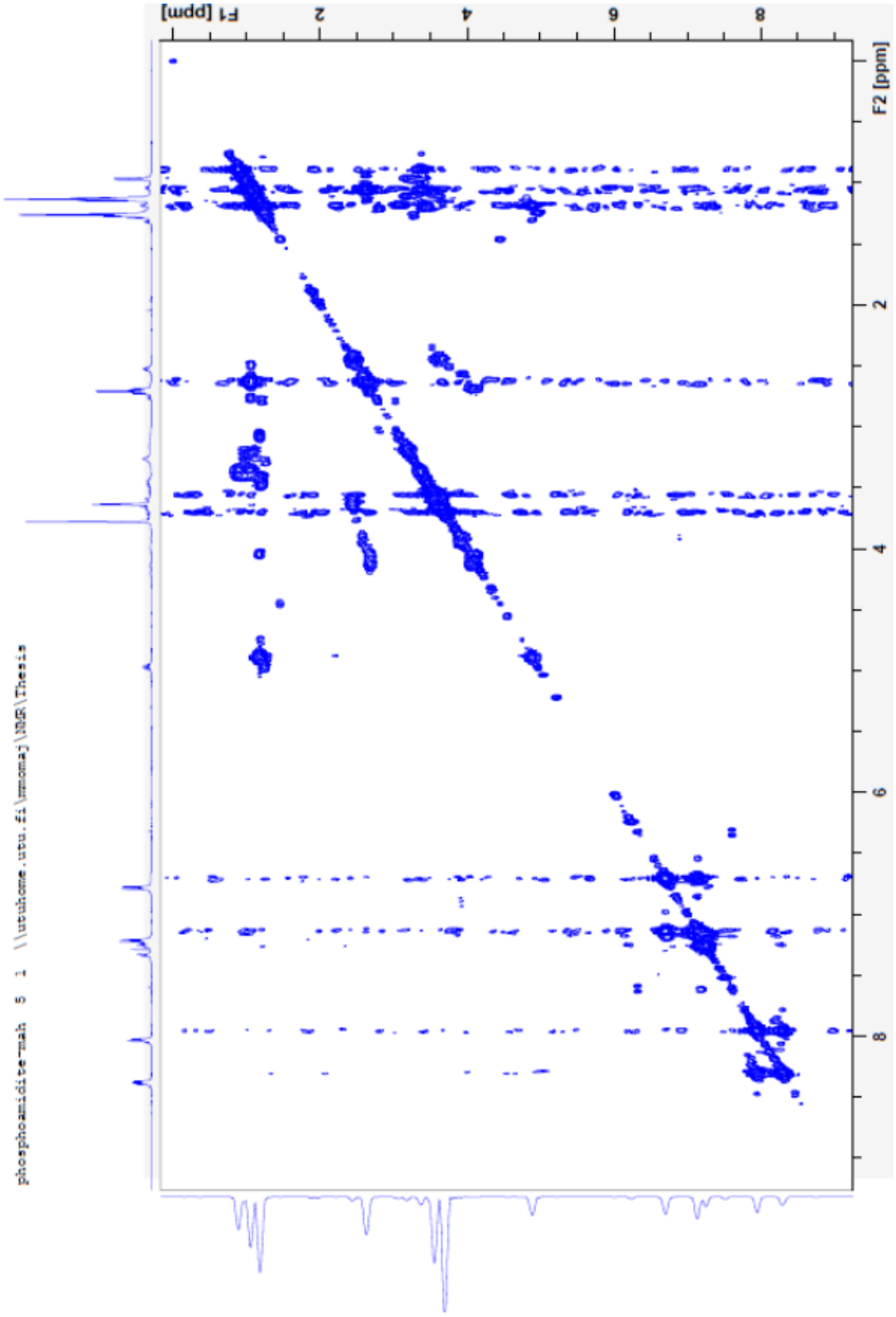

Figure 16 COSY spectrum of phosphoramidite **8**

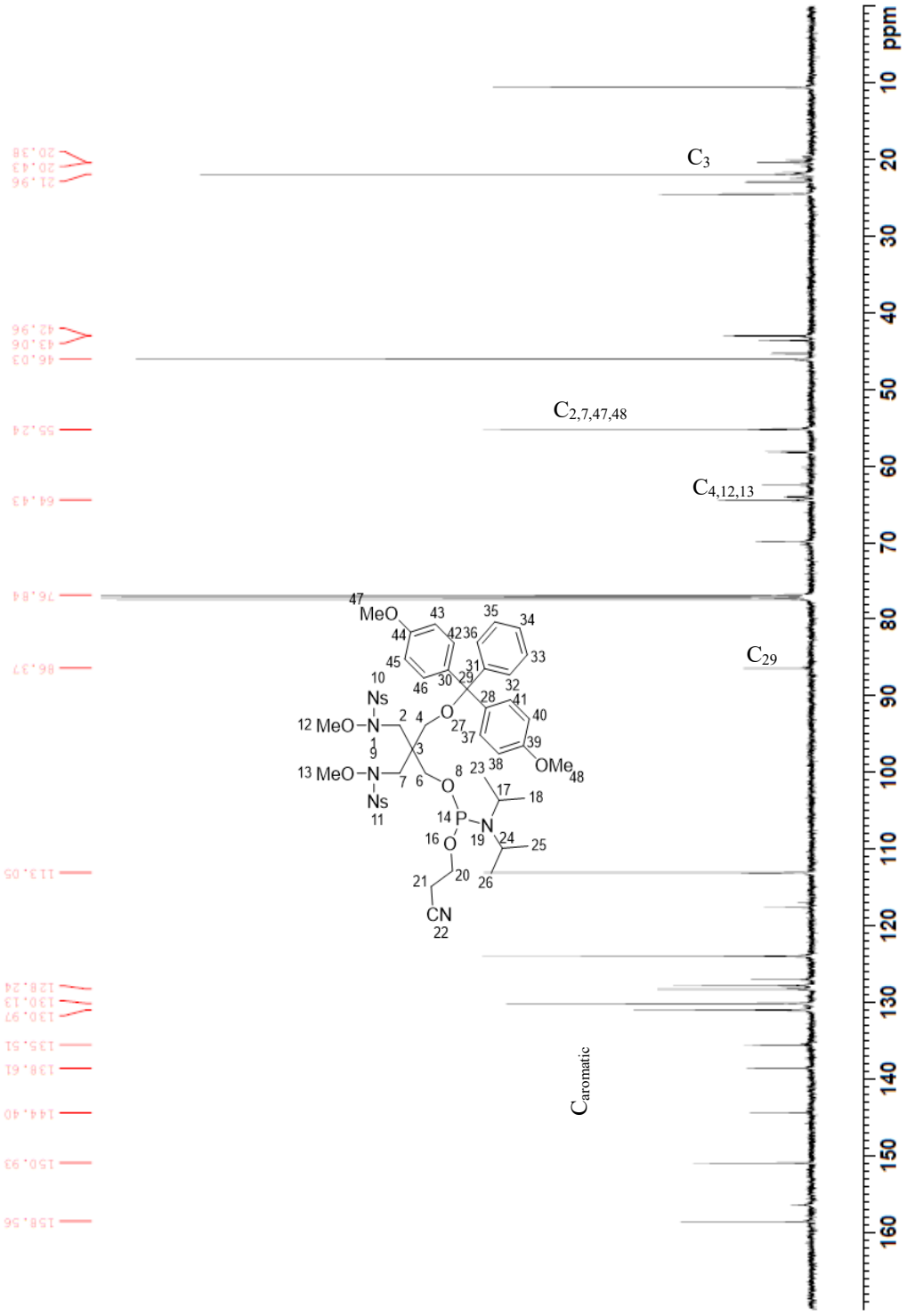

Figure 17 ^{13}C NMR spectrum of phosphoramidite **8**

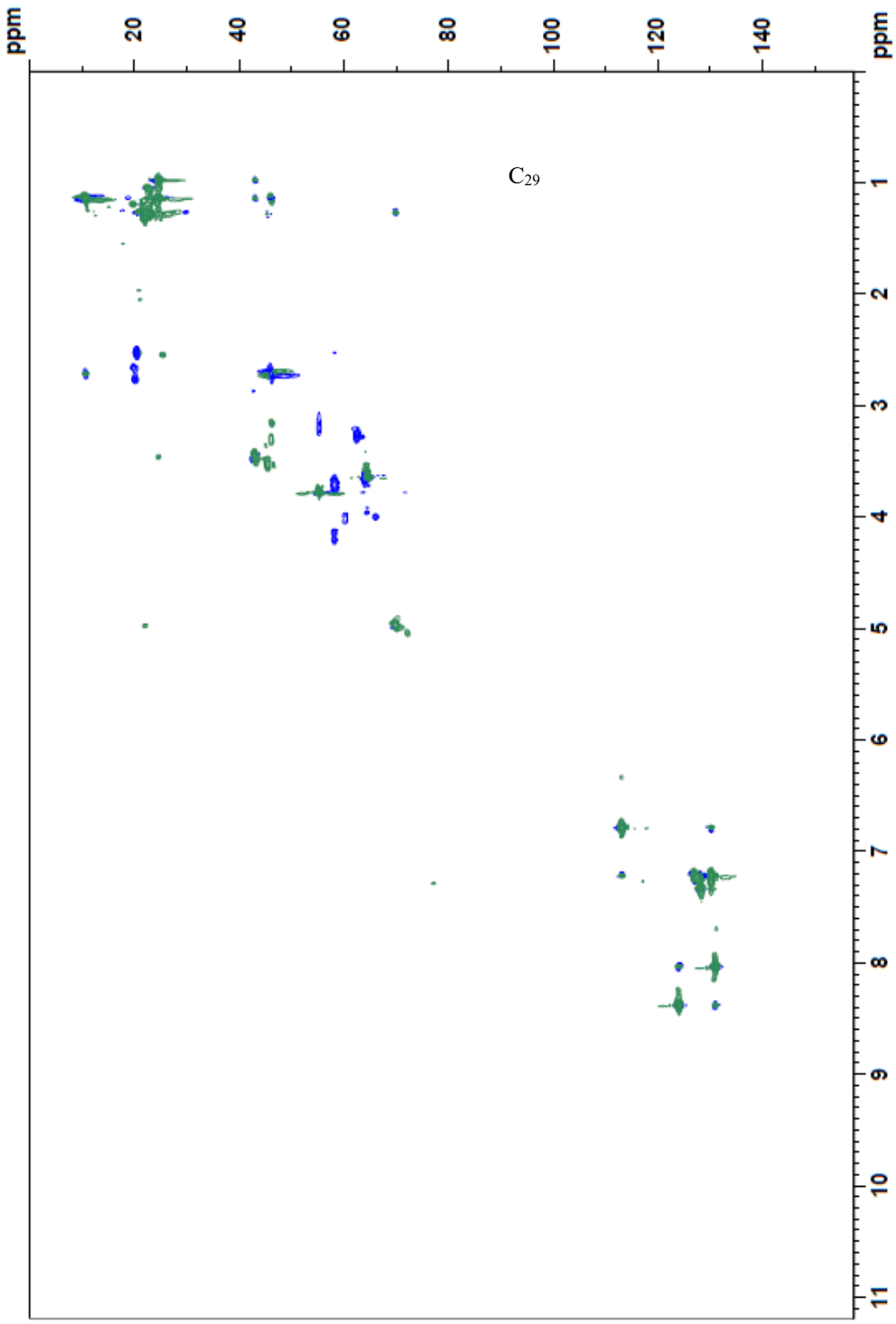

Figure 18 HSQC spectrum of Compound 8

Figure 19 ^{31}P NMR spectrum of phosphoramidite **8**

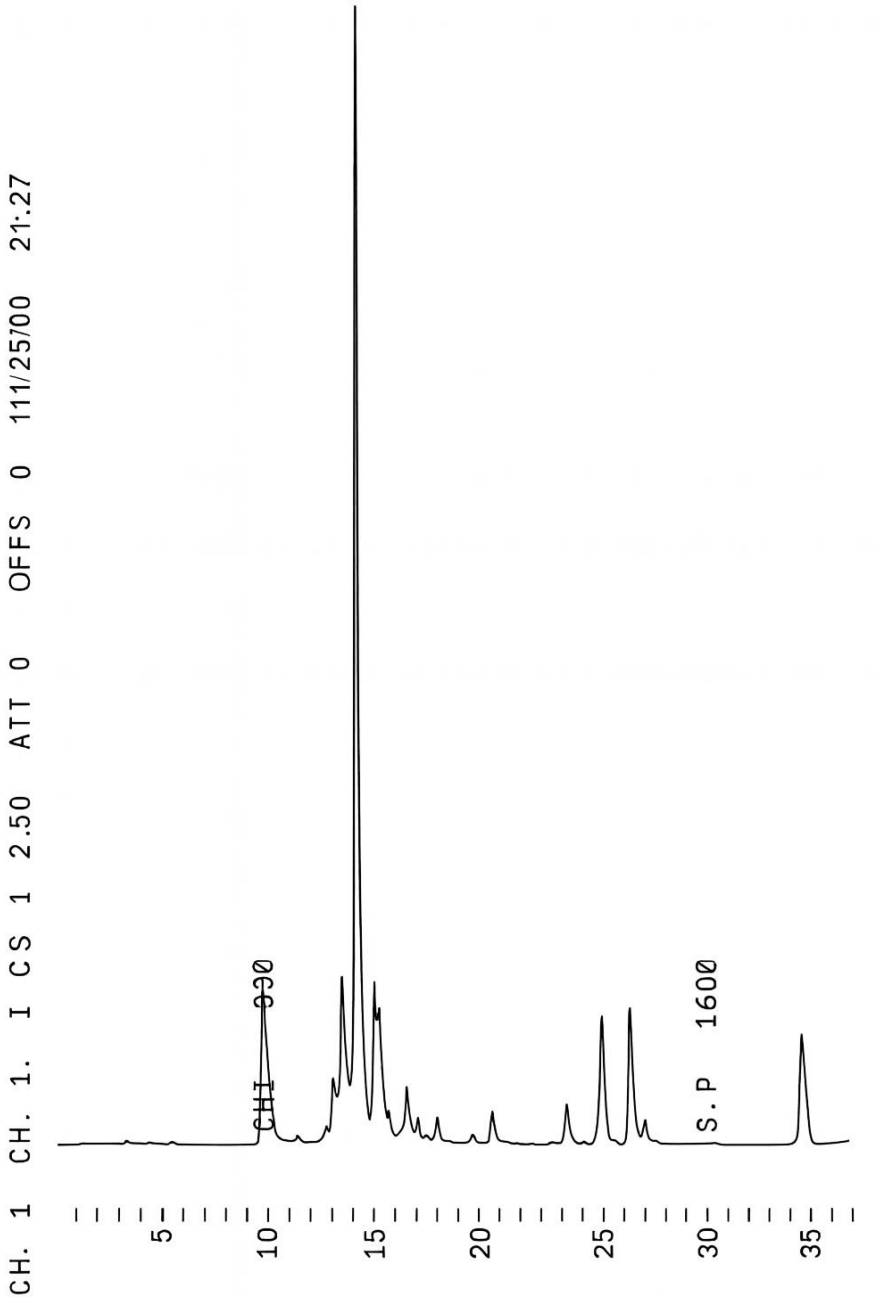

Figure 20 HPLC Chromatogram of the interchain-modified oligonucleotide synthesis reaction mixture after ammonolysis-

The chromatogram quality is enhanced using AI-based image processing

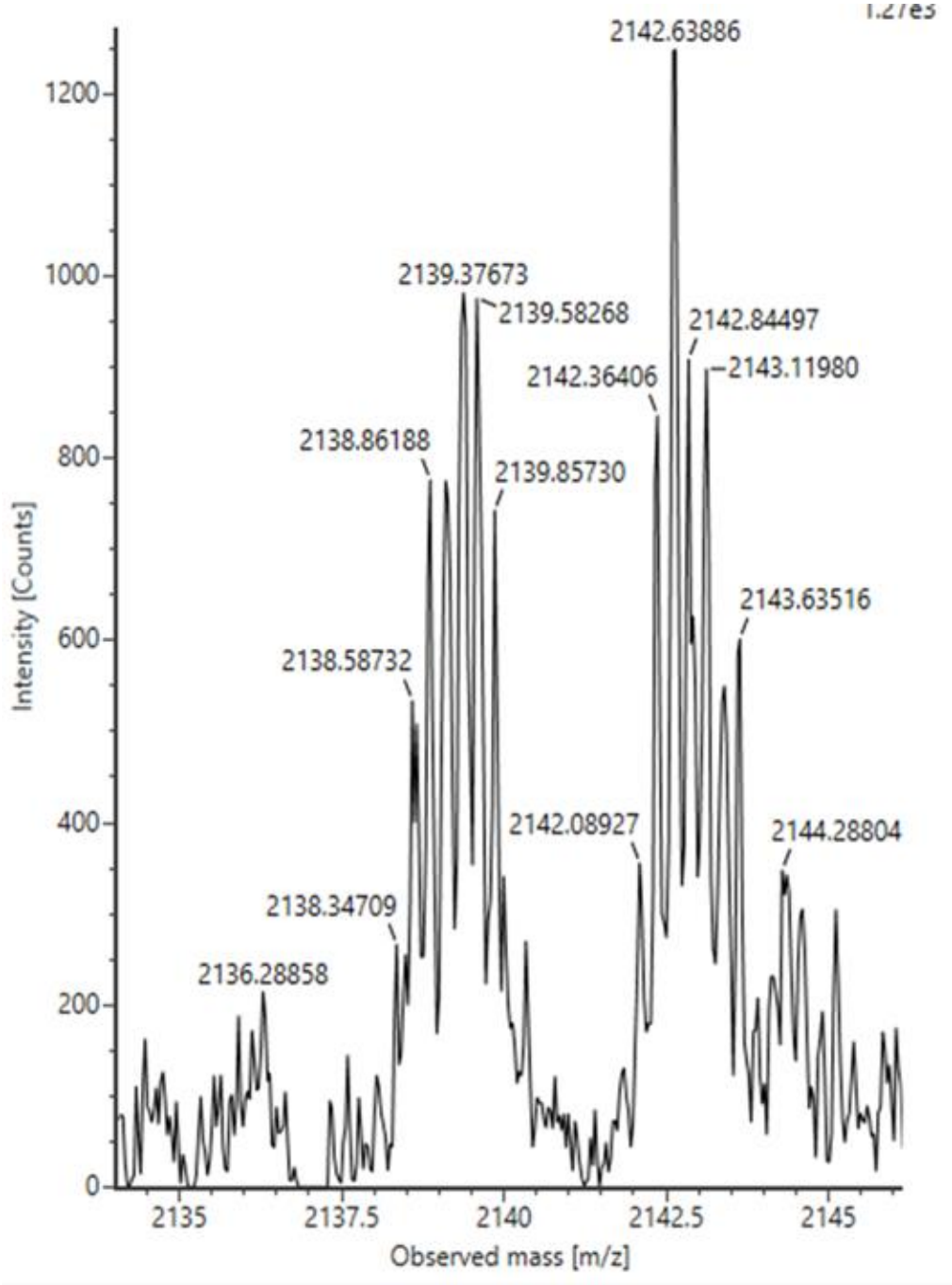

Figure 21 ESI-TOF HRMS of compound **11**, m/z : 2139.38 Da for $[M-4H]^{4-}$formaldehyde adduct m/z: 2142.64 Da for $[M-4H]^{4-}$ acetaldehyde adduct

The spectrum quality is enhanced using AI-based image processing